

# Developing a Colorimetric, Magnetically Separable Sensor for the Capture and Detection of Biomarkers

by

Terence Chan

A thesis  
presented to the University of Waterloo  
in fulfillment of the  
thesis requirement for the degree of  
Master of Applied Science  
in  
Chemical Engineering

Waterloo, Ontario, Canada, 2012

©Terence Chan 2012

## **AUTHOR'S DECLARATION**

I hereby declare that I am the sole author of this thesis. This is a true copy of the thesis, including any required final revisions, as accepted by my examiners.

I understand that my thesis may be made electronically available to the public.

## Abstract

Point-of-care testing (POCT) devices have received increasing attention because of their potential to address the urgent need for quick and accurate diagnostic tools, especially in areas of personal care and clinical medicine. They offer several benefits over current diagnostic systems, including rapid diagnostic results in comparison to microbial cultures, simple interpretation of results, portability, and requiring no specialised laboratory equipment or technical training to operate. These are essential for diagnosing critical illnesses, such as sepsis, in areas of poor healthcare infrastructure. Sepsis, an innate physiological response to infection, is a growing problem worldwide with high associated costs and mortality rates, and affects a wide range of patients including neonates, infants, the elderly, and immunocompromised individuals.

A literature review of the biomarkers of sepsis and the currently available diagnostic systems indicates the need for a biosensor capable of meeting the requirements of designing POCT systems and achieving detection of low concentrations of biomarkers. To meet these demands, two significant contributions to developing POCT platforms have been achieved and described in this thesis, including: 1) development of a colorimetric, magnetically separable biosensor that can be easily fabricated and demonstrates an easily identifiable colour response upon analyte detection, as well as the ability to capture and detection target biomarkers at low concentrations from complex solutions; and 2) tuning of the biosensor's colorimetric response to achieve low detection limits, as well as demonstration of the versatility of the biosensor for sensing different target analytes. The developed biosensor in this work combines colour responsive polydiacetylenes and superparamagnetic iron oxide for the first time to achieve a biosensor capable of meeting these demands. The sensors exhibit identifiable colour responses to biomolecule detection, capture of a target analyte from complex solutions, sensing of different target analytes, a lower detection limit of 0.01 mg/mL, and rapid separation from solution with a common magnet. This work has been a significant demonstration of the capabilities of this biosensor as a new platform for POCT systems to diagnosis sepsis, and potentially other sensing applications.

## **Acknowledgements**

I would like to acknowledge my supervisor Frank Gu and the members of the Frank Gu Research Group for their ongoing support throughout this project, especially Mohit Verma and Tim Leshuk for their advice, as well as Dale Weber for his expertise on transmission electron microscopy.

## **Dedication**

I dedicate this thesis to my family, especially my mom, for their extraordinary love and sacrifice to support my continuing education.

## Table of Contents

AUTHOR'S DECLARATION .....	ii
Abstract .....	iii
Acknowledgements .....	iv
Dedication .....	v
Table of Contents .....	vi
List of Figures .....	viii
List of Tables .....	ix
1.0 Introduction .....	1
1.1 Point-of-care testing .....	1
1.2 Sepsis .....	1
2.0 Literature Review .....	3
2.1 Biomarkers of sepsis .....	3
2.2 Biomarkers for bacterial causes of sepsis .....	4
2.2.1 C-reactive protein .....	4
2.2.2 Procalcitonin .....	5
2.2.3 Serum amyloid A .....	6
2.3 Biomarkers for fungal causes of sepsis .....	6
2.4 Biomarkers for viral causes of sepsis .....	7
2.5 Other biomarkers requiring further research .....	8
2.6 Currently available assays .....	9
2.6.1 Assays for C-reactive protein .....	9
2.6.2 Assays for procalcitonin and serum amyloid A .....	10
2.6.3 Assays for mannan and anti-mannan .....	12
2.6.4 Assays for interferon- $\gamma$ -inducible protein 10 .....	12
2.7 Commentary on sepsis biomarker research .....	13
2.8 Five year outlook .....	14
3.0 Research objectives .....	16
3.1 Sensor development for biomolecule detection objectives .....	16
3.2 Sensor tuning objectives .....	17
4.0 Development of a Colorimetric, Superparamagnetic Biosensor for the Capture and Detection of Biomolecules .....	19

4.1 Introduction .....	19
4.2 Experimental Methods.....	20
4.2.1 Synthesis of hydrophobic superparamagnetic iron oxide nanoparticles.....	20
4.2.2 Amphiphilic modification of diacetylene monomer.....	21
4.2.3 Fabrication of Lys-PCDA/SPION core-shell particle .....	21
4.2.4 Detection of anti-bovine serum albumin antibodies.....	21
4.3 Results and Discussion .....	22
4.3.1 Characterisation of Lys-PCDA/SPION-based biosensors.....	22
4.3.2 Colorimetric performance of Lys-PCDA/SPION sensors.....	23
4.4 Conclusions .....	26
5.0 Optimisation of polydiacetylene-coated superparamagnetic iron oxide for colorimetric detection and capture of biomarkers .....	27
5.1 Introduction .....	27
5.2 Experimental Methods.....	27
5.2.1 Materials.....	27
5.2.2 Synthesis.....	28
5.2.3 Biosensor fabrication.....	28
5.2.4 Antibody assay .....	28
5.2.5 Characterisation.....	28
5.3 Results and discussion.....	29
5.3.1 Optimisation of polydiacetylene amount used in sensor fabrication.....	29
5.3.2 Optimisation of colorimetric biomolecule detection .....	32
5.4 Conclusions .....	37
6.0 Conclusions and Recommendations.....	38
6.1 Concluding Summary.....	38
6.2 Recommendations for Future Work.....	39
Appendix A .....	40
Permissions.....	45
Bibliography.....	46

## List of Figures

<b>Figure 1. A possible strategy for diagnosing the type of infectious cause of sepsis .....</b>	<b>14</b>
<b>Figure 2. Schematic representation of colorimetric, magnetically separable functionalised Lys-PCDA/SPION particles, describing the capturing and sensing of a target biomolecule from a complex solution .....</b>	<b>20</b>
<b>Figure 3. Demonstration of the colorimetric and magnetic properties of Lys-PCDA/SPIONs...</b>	<b>23</b>
<b>Figure 4. Biosensor performance of BSA-functionalised Lys-PCDA/SPIONs .....</b>	<b>25</b>
<b>Figure 5. Characterisation of Lys-PCDA/SPION sensors .....</b>	<b>31</b>
<b>Figure 6. Photographs of Lys-PCDA/SPION sensors of varying PDA wt%.....</b>	<b>32</b>
<b>Figure 7. Absorption spectra of Lys-PCDA/SPION sensors of varying PDA wt%, normalised to 650 nm .....</b>	<b>33</b>
<b>Figure 8. Absorption spectra of Lys-PCDA/SPION sensors of 80-95 wt% PDA, normalised to 650 nm, in increasing horse IgG concentrations.....</b>	<b>34</b>
<b>Figure 9. Absorption spectra of Lys-PCDA/SPION sensors of 60-75 wt% PDA, normalised to 650 nm, in increasing horse IgG concentrations.....</b>	<b>35</b>
<b>Figure 10. Colorimetric response of 85, 90 and 95 wt% PDA compositions of Lys-PCDA/SPION sensors, normalised against the colorimetric response at 0.01 mg/mL horse IgG.....</b>	<b>36</b>

## List of Tables

<b>Table 1. Summarising the components of diagnostic accuracy of a biomarker. ....</b>	<b>3</b>
<b>Table 2. Reported diagnostic accuracy values of C-reactive protein, procalcitonin, serum amyloid A, mannan, anti-mannan, and interferon-<math>\gamma</math>-inducible protein 10. ....</b>	<b>8</b>
<b>Table 3. Available assays measuring CRP. ....</b>	<b>10</b>
<b>Table 4. Available assays measuring procalcitonin. ....</b>	<b>11</b>
<b>Table 5. Available assays measuring serum amyloid A. ....</b>	<b>12</b>

## 1.0 Introduction

### 1.1 Point-of-care testing

The past decade in diagnostics has seen an increasing demand for point-of-care testing (POCT) devices to address the urgent need for quick and accurate diagnostic tools, especially in areas of personal care and clinical medicine. Existing rapid and/or automated diagnostic systems used in the clinical setting are based on molecular sensing-techniques, such as such as enzyme-linked immunosorbent assay, polymerase chain reaction, and fluorescence *in situ* hybridisation. The molecules targeted are termed biomarkers, which are best described as “a characteristic that is objectively measured and evaluated as an indicator of normal biologic processes [or] pathogenic processes”.<sup>1</sup> These biomarker-based diagnostic systems typically operate by monitoring abnormal changes in specific biomarker concentrations found in bodily fluids, which are indicative of a disease state.

Similar to existing rapid molecular-based diagnostic systems, point-of-care testing devices are biomarker-based systems designed to produce quick diagnostic results, ideally within several minutes to under an hour. In addition, POCT devices offer several advantages over existing rapid diagnostic systems, including: requiring no expertise or specialised training to operate; providing easily interpretable diagnostic results; being extremely portable and self-contained; and requiring no complex or technique-dependent manipulations of the samples.<sup>2-4</sup> These features become inherently useful in rural and low income communities and other areas of poor healthcare infrastructure, where specialised laboratory equipment and highly trained technicians are commonly not available. POCT systems have the potential to perform similarly to lab diagnostic techniques and have been previously demonstrated to this effect in the clinical field, such as the early diagnosis of HIV patients when compared to a flow cytometry technique in the laboratory setting.<sup>5</sup> Ideal POCT devices should also be relatively simple to manufacture if their target usage is in rural and low income communities. Consequently, the practicality of such devices extends beyond medicine to other applications ranging from food safety to hazardous material detection.

### 1.2 Sepsis

In clinical medicine, point-of-care testing devices are critically needed for diagnosing diseases with rapidly-developed adverse effects. One such disease is sepsis, which is a growing worldwide problem worldwide and associated with a mortality rate as high as 60%.<sup>6,7</sup> Although

sepsis is not a true disease but rather an innate physiological response by the immune system to infection,<sup>8</sup> it is estimated that severe sepsis affects over 750,000 people in the United States alone each year, resulting in an annual cost of almost \$17 billion,<sup>9</sup> underscoring the costly consequences of sepsis. It is a highly detrimental problem for those with weakened immune systems, including infants,<sup>10-14</sup> the elderly and immunocompromised and critically ill patients.<sup>15</sup> Sepsis remains a common and similarly expensive problem in developing nations, where sepsis is known to affect up to every 30 of 1000 live births.<sup>16, 17</sup>

Most studies define sepsis as a systemic inflammatory response to bacterial, fungal, or viral infections.<sup>8, 18</sup> In the clinical setting, several other physiological symptoms must be presented to diagnose sepsis, which often delays the diagnosis of sepsis.<sup>19-21</sup> As a result, the common treatment for patients suspected of sepsis is the administration of broad spectrum antimicrobials.<sup>22, 23</sup> The gold standard of diagnosing sepsis has traditionally been the use of microbial cultures to identify the source of illness.<sup>6, 17</sup> However, the major limitation of using cultures is the length of time required to develop cultures to identifiable quantities. Cultures are also reported to be insensitive under several conditions,<sup>24-28</sup> including slow growing and non-cultivable microorganisms and microorganisms present at very low concentrations. In light of these limitations and the widespread problem of sepsis in developing nations, POCT devices are ideal systems for the diagnosis of sepsis.

This thesis describes the work done in the development of a colorimetric, magnetically separable sensor for future applications in point-of-care testing systems, specifically for the diagnosis of sepsis. Before describing the project design and its objectives, a comprehensive literature review of the most commonly studied sepsis biomarkers that are directly quantifiable from human serum is presented, since POCT devices operate with minimal sample manipulation. An overview of commercially available diagnostic systems used for sepsis biomarkers is also provided to identify the needs not fulfilled by current devices.

## 2.0 Literature Review

The following literature review has been published in Expert Review of Molecular Diagnostics, June 2011, volume 11, issue 5, pages 487-96, authored by Terence Chan and Frank Gu, adapted with permission of Expert Reviews Ltd.

### 2.1 Biomarkers of sepsis

To be considered clinically relevant, a biomarker must have high diagnostic accuracy (DA).<sup>29</sup> It must have high sensitivity, specificity, positive predictive value (PPV), and negative predictive value (NPV) (Table 1). Many biomarkers also calculate the likelihood ratio (LR) to determine if test results are truly indicative of disease or due to random chance. Indicators such as the positive and negative likelihood ratios, which are calculated based on sensitivity and specificity, are also useful for assessing the strength of a diagnostic test. It is commonly graphed for multiple cutoff values as a receiver operating characteristic curve. The area under the curve (AUC) value is used to determine the best diagnostically relevant cutoff value (CV). At a CV where the AUC is equal to 1, an ideal biomarker would possess 100% sensitivity, specificity, PPV, and NPV.

Since sepsis can be caused by bacterial, fungal, and viral infections, the biomarkers reviewed are categorised based on their most common diagnostic usage.

**Table 1. Summarising the components of diagnostic accuracy of a biomarker.**

Diagnostic measure	Definition	100% indicates
Sensitivity	$\frac{\text{True Positives}}{\text{True Positives} + \text{False Negatives}}$	All detected diseased samples are truly diseased
Specificity	$\frac{\text{True Negatives}}{\text{True Negatives} + \text{False Positives}}$	All detected healthy samples are truly healthy
Positive predictive value	$\frac{\text{True Positives}}{\text{True Positives} + \text{False Positives}}$	Only truly diseased samples are detected as diseased
Negative predictive value	$\frac{\text{True Negatives}}{\text{True Negatives} + \text{False Negatives}}$	Only truly healthy samples are detected as being healthy
Positive likelihood ratio	$\frac{\text{Sensitivity}}{1 - \text{Specificity}}$	Ratio specifies that a positive test outcome is more likely to indicate a diseased state.
Negative likelihood ratio	$\frac{1 - \text{Sensitivity}}{\text{Specificity}}$	Ratio specifies that a negative test outcome is more likely to indicate a non-diseased state.

## 2.2 Biomarkers for bacterial causes of sepsis

### 2.2.1 C-reactive protein

C-reactive protein (CRP) is a general acute-phase reactant protein that rises in concentration up to 1000-fold in the blood in response to inflammation and infection.<sup>1, 20, 23, 29-34</sup> Sensitivity values have been reported from 30-97.2%, specificity of 75-100%, PPV of 31-100%, and NPV of 81-97% (Table 2).<sup>11, 23, 30, 32, 35-39</sup> The large disparity in diagnostic accuracy values is mainly due to the wide range of cutoff values used in different studies, ranging from 0.2-110 mg/L. The rapid improvement of assays used in studies to detect CRP has also dramatically affected the determined CVs. A 2003 study on neonates reported a CV of 40 mg/L when using the NycoCard CRP test,<sup>39</sup> whereas a 2010 study on neonates using the automated immunoassay IMx system reported CVs of 0.2-0.6 mg/L.<sup>38</sup>

The variation in results can also be caused by the use of different assays. Each assay has a unique functional detection limit. Among the 15 different studies reviewed that measured CRP and mentioned the equipment used, 10 different assay systems from various manufacturers were used. The variation in equipment also reflects the various different study designs between studies. While some studies focus on neonates,<sup>11, 19, 30, 35, 37, 39-41</sup> others focus on children,<sup>31, 35-37, 39, 42, 43</sup> adults,<sup>31, 32, 41, 44-48</sup> and the elderly.<sup>25, 31, 38, 41</sup> Serum CRP levels also vary with age in healthy individuals.<sup>41</sup> The authors of the study suggested that a CV of 10 mg/L be used for elderly patients over 65, while a CV of 5 mg/L should be used for adults and infants between 3-7 days old. CRP levels are also naturally higher in older children compared to younger children.<sup>42</sup>

Studies have shown CRP to be highly sensitive<sup>11, 25, 37, 39, 44</sup> or highly specific<sup>30, 35</sup> for infection. However, it is unclear if CRP can be used to distinguish Gram positive from Gram negative bacterial infections.<sup>44</sup> CRP is also studied as a diagnostic marker for other illnesses.<sup>23, 38, 47, 49, 50</sup> A recent study on community-acquired pneumonia (CAP) showed CRP as a prognostic marker in determining the severity of CAP and the need for hospitalisation when using a CV of 110 mg/L.<sup>38</sup> CRP is also reported to distinguish bacterial from fungal infections, where levels above 100 mg/L are indicative of bacterial infection and elevated levels below 100 mg/L are indicative of fungal infection.<sup>25, 45</sup> Several studies have examined the diagnostic relevancy of CRP in viral infections,<sup>47, 51, 52</sup> and current data suggests that CRP is an unreliable marker for viral infections on its own.<sup>47, 52</sup>

## 2.2.2 Procalcitonin

Procalcitonin (PCT), a precursor to the hormone calcitonin, is another candidate biomarker for bacterial infection. It is reported to be present at very low concentrations of 0.033 ng/mL in the serum of healthy individuals,<sup>21</sup> and is known to increase by up to 1000-fold under inflammatory conditions.<sup>21, 53-55</sup> It is reported to rise within 2-4 hours of infection and peak at 6-8 hours.<sup>10, 19, 54</sup> Persistent elevated levels are indicative of the continual presence of infection or sepsis.<sup>21</sup> The rapid upregulation and sustainment of PCT levels in the serum during infection makes it an ideal biomarker. It is also a stable molecule, an important biomarker quality, remaining stable during blood preparation methods and freezing procedures and after long-term storage.<sup>37, 56, 57</sup>

PCT has been shown to have high diagnostic accuracy, reporting sensitivity values of 74.8-100%, specificity values of 70-100%, PPV of 55-100%, and NPV of 56.3-100% (Table 2).<sup>10, 15, 25, 32, 36, 37, 39, 53</sup> Similar to the studies on CRP, the variation in diagnostic accuracy values can also be explained by variations in cutoff values, equipment used, and study designs. Although many studies have used a cutoff value of 0.5 ng/mL, a range of CVs have been reported (Table 2). A 2001 study on critically ill children with sepsis reported a CV of 8.05 ng/mL, using an immunoluminometric assay available at the time.<sup>39</sup> In comparison, a 2009 study on critically ill children with sepsis determined a CV of 0.28 ng/mL, using the newer immunoluminometric LIAISON BRAHMS PCT assay.<sup>35</sup>

As a biomarker for bacterial infection, most studies find PCT to be a useful and accurate biomarker<sup>19, 21, 58-61</sup> and more useful than other common inflammatory markers.<sup>25, 32, 36, 39, 42, 53, 62</sup> Several studies have reported significantly elevated levels of PCT in patients with sepsis compared to those without sepsis.<sup>15, 21, 23, 25, 26, 31, 46, 53, 54, 63</sup> Studies have also reported PCT being used as a prognostic marker, indicating that levels of PCT are a good indicator of response to treatment,<sup>54, 62, 64, 65</sup> severity of sepsis,<sup>25, 54</sup> and mortality from sepsis.<sup>31, 54, 66</sup> Similar to the case of CRP, it is unclear if PCT can be used to distinguish between Gram positive and Gram negative bacterial infections,<sup>21, 32, 62</sup> which are treated with different strategies.

PCT has also been used to distinguish fungal and viral infections from bacterial infections. During viral infections, PCT levels are reported to remain at low levels, often at concentrations found in healthy individuals.<sup>21, 54, 64</sup> A study on 122 children with viral infection reported that the maximum PCT level observed was 0.7 ng/mL.<sup>67</sup> PCT can also be used to differentiate bacterial from viral meningitis.<sup>54, 61</sup> In comparison, fungal infections tend to cause mild elevations in PCT concentration compared to levels seen in bacterial infections.<sup>21, 25, 45, 53, 54, 62</sup> Studies on invasive aspergillosis and

invasive candidiasis have reported significantly higher levels of PCT in patients with bacterial sepsis than those with fungal infection.<sup>25, 45</sup> PCT also shows potential as a diagnostic marker for pneumonia, abdominal infections, urinary tract infections, lower respiratory tract infections, and myocardial infarction.<sup>49, 54, 56, 59, 64, 65, 68</sup> It has also been demonstrated as a biomarker to guide antibiotic therapy in patients with CAP.<sup>29, 55, 62, 65, 69, 70</sup>

### **2.2.3 Serum amyloid A**

Serum amyloid A (SAA) is an apolipoprotein reported to have potential for diagnosing sepsis.<sup>10, 30</sup> SAA is expressed up to 1000 times higher in 8-24 hours of sepsis.<sup>10, 71</sup> Compared to CRP levels, SAA levels are reported to rise faster and higher after the onset of sepsis and remain at higher relative elevations.<sup>30</sup> Similar to PCT and CRP, studies using SAA have reported various diagnostic accuracy values and cutoff values (Table 2), likely a result of the different assays used, as well as the development of assays with lower detection limits. Serum SAA levels of <15 mg/L for the elderly over 65 and <10 mg/L for adults and newborns aged 3-7 days are indicative of healthy states.<sup>23</sup>

Although SAA is mainly studied as a biomarker for bacterial infection, a recent study on patients with viral infections reported elevated SAA levels above the healthy cutoff of 10 mg/L among the infected patients.<sup>47</sup> However, SAA may not be clinically useful because it was too sensitive, as it was reported in the same study to increase during minor viral infections and in patients not presenting symptoms.

## **2.3 Biomarkers for fungal causes of sepsis**

Mannan and anti-mannan antibodies (M+AM) are used exclusively to diagnose invasive fungal infections, due to the presence of mannan in the cell walls of the invasive fungal organisms.<sup>28</sup> M+AM levels are elevated in blood during invasive fungal infections,<sup>45</sup> such as candidiasis and aspergillosis, making them potentially useful biomarkers for diagnosing fungal causes of sepsis. Reported diagnostic accuracy values and cutoff values for M+AM vary between studies, and are either measured as separate biomarkers<sup>45, 72</sup> or in combination<sup>72, 73</sup> (Table 2). It has been reported that combining mannan and anti-mannan tests provides the best diagnostic accuracy values.<sup>72</sup> Similar to the biomarkers used for bacterial infections, DA value variations are likely due to the different assays and study methodologies. Assays with lower detection limits are also required, as all three studies reviewed reported cutoff values lower than the manufacturer's suggested diagnostic CVs.

The main disadvantage of using M+AM tests alone is the high rate of false-positives and false-negatives that mannan assays produce,<sup>28</sup> requiring that these tests be used in conjunction with other diagnostic tests.  $\beta$ -D-glucan (BDG) tests have been used in combination with M+AM tests since BDG tests are highly sensitive and specific for invasive mycosis, and not species specific.<sup>28, 73</sup> Using M+AM as biomarkers also requires frequent serial measurements, as mannan is cleared relatively quickly from the blood.<sup>28, 74</sup>

## **2.4 Biomarkers for viral causes of sepsis**

Interferon- $\gamma$ -inducible protein 10 (IP-10), a proinflammatory chemokine, is a promising a biomarker for diagnosing viral infections due to its role in the host response to viral infections.<sup>75</sup> A recent study on bacterial infections in very low birth weight infants concluded that IP-10 could be a good diagnostic marker during initial measurements, reporting significant elevated IP-10 levels in infected patients at both initial and 24 hour measurements, with no overlap of ranges. IP-10 levels may also correlate with the severity of infection.<sup>75</sup>

Differences in diagnostic accuracy values and cutoff values exist between IP-10 studies<sup>52, 75, 76</sup> (Table 2), a result of the complex nature of viral infections. The large variety of viral illnesses means studies must focus on a specific virus infection, requiring very specific study populations and assays. However, current studies report IP-10 to be a potentially useful biomarker.<sup>52, 75, 76</sup> It is known from previous studies that IP-10 is released in response to viruses such as rhinovirus, RSV, hepatitis B and C viruses, and H5N1 influenza.<sup>76, 77</sup> In addition, IP-10 in the serum has been shown as a prognostic marker in guiding treatment in hepatitis C patients.<sup>78</sup>

**Table 2. Reported diagnostic accuracy values of C-reactive protein, procalcitonin, serum amyloid A, mannan, anti-mannan, and interferon- $\gamma$ -inducible protein 10.**

Biomarker	Cutoff Value	Diagnostic Accuracy Values (%)				Studies
		Sensitivity	Specificity	PPV	NPV	
CRP	1.56-110 mg/L	30-97.2	75-100	31-100	81-97	11, 23, 30, 32, 35-39
PCT	0.3-8.05 ng/mL	74.8-100	70-100	55-100	56.3-100	10, 15, 25, 32, 36, 37, 39, 53
SAA	8-68 mg/L	76.4-98.4	92.3-100	85-100	58-99	10, 30, 39
Mannan	0.1-1 ng/mL	67-78	73-100	58-100	72.7-87	45, 72
M+AM	0.1-0.25 ng/mL; 2.6-4 AU/mL*	73-100	73.9-80	36-80	95-100	72, 73
IP-10	260-1700 pg/mL	67-93	59.4-89	77**	97**	52, 75, 76

Note: AM – anti-mannan; AU – arbitrary units; CRP – C-reactive protein; IP-10 – interferon- $\gamma$ -inducible protein 10; M – mannan; NPV – negative predictive value; NS – not stated; PCT – procalcitonin; PPV – positive predictive value; SAA – serum amyloid A; \* – cutoff value for AM; \*\* – reported only by one study.

## 2.5 Other biomarkers requiring further research

Interleukin 10 (IL-10) is a potentially useful biomarker of sepsis. IL-10 is reported to be a promising diagnostic marker of both early- and late-onset sepsis among neonates, where a cutoff value of >17.3 pg/mL resulted in respective diagnostic accuracy values of 92%, 84%, 80%, and 89%.<sup>20</sup> A study on very low birth weight infants found IL-10 to be one of only three markers with diagnostically relevant sensitivity and specificity values ( $\geq 80\%$ ) when using a CV of 7.6 pg/mL for late-onset sepsis.<sup>75</sup> In general, circulating cytokines, such as interleukins, have a short half-life, which can result in false negatives, ultimately limiting their diagnostic accuracy.<sup>19, 30</sup>

A potentially useful biomarker specific to bacterial infections is lipopolysaccharide binding protein (LBP). Serum LBP levels are known to increase during bacterial and fungal infections, but not viral infections.<sup>79</sup> A study on critically ill neonates and children with sepsis reported LBP to be a better biomarker for sepsis than PCT, CRP, and soluble CD14.<sup>79</sup> Soluble triggering receptor expressed on myeloid cells-1 (sTREM-1) is another potential biomarker, as it is not upregulated during non-infectious inflammatory diseases,<sup>65</sup> a property not found in other biomarkers like PCT. A

recent study reported significantly elevated plasma sTREM-1 levels in sepsis patients compared to SIRS patients and found it to be a diagnostically accurate biomarker.<sup>46</sup>

Toll-like receptor 2 (TLR-2) and neutrophil CD64 receptor (nCD64) are two potentially useful biomarkers only present on cell surfaces. During infection, both experience upregulated expression on the surface of monocytes<sup>47</sup> and neutrophils,<sup>35, 80</sup> respectively. A recent study found significantly elevated TLR-2 expression during viral and bacterial infections.<sup>47</sup> The study used patients with influenza A and B, RSV, mumps, varicella-zoster virus, and cytomegalovirus, indicating TLR-2 could be a potential biomarker of viral infections. nCD64 has been widely used as a sensitive biomarker of bacterial infection in settings that allow for laboratory testing.<sup>81</sup> nCD64 expression is not affected by underlying or inflammatory diseases and is not differentially expressed between systemic and local bacterial infections.<sup>80</sup> Although different studies have used differing units to calculate the CVs, the DA values reported for nCD64 are generally diagnostically relevant. For example, reported sensitivity values range from 71-97%, 71-100% for specificity, 53-100% for PPV, and 75.9-98% for NPV.<sup>15, 20, 35, 80, 82, 83</sup>

## **2.6 Currently available assays**

### **2.6.1 Assays for C-reactive protein**

Various assays have been designed for measuring CRP, briefly summarised in Table 3.

**Table 3. Available assays measuring CRP.**

Assay	Manufacturer	Lower detection limit <sup>‡</sup>	Sample used	Study used
IMx system	Abbott Laboratories	0.05 mg/L <sup>a</sup>	Serum	40
BN II analyzer	Dade Behring	5 mg/L	Serum	10
BN ProSpec analyzer	Dade Behring	0.16 mg/L	Serum	23, 41
CRPLX Tina-quant kit	Roche-Hitachi	0.4 mg/L	Serum	30, 38, 43, 66
Advia 1650 analyzer	Bayer HealthCare Diagnostics	N/A	Serum	48
Micros CRP 200	Horiba Medical	2 mg/L <sup>b</sup>	Serum	43
automated turbidmetric analyzer	Boehringer-Mannheim	3 mg/L	Serum	35
Vitros 250 Dry Chemistry System	Ortho-Clinical Diagnostics	7 mg/L	Plasma	42
QuickRead CRP	Orion Diagnostica	8 mg/L	20 µl of whole blood	11
NycoCard CRP	Axis-Shield PoC AS	8 mg/L	5 µl of whole blood	11, 36, 37

Note: <sup>‡</sup> - if functional sensitivity values were not made available, the reported lower detection limits are listed, which may be lower than the functional sensitivity values; <sup>a</sup> - stated in [90]; <sup>b</sup> - stated on manufacturer's website; N/A - not available.

QuickRead CRP, an immunoturbidometric assay, and NycoCard CRP, a chromatographic immunometric assay, are especially interesting for diagnostics purposes because of the fast run times. A recent study compared the two CRP assay kits on neonates with sepsis.<sup>11</sup> Using a CV of 10 mg/L for both kits, the QuickRead CRP kit produced diagnostic accuracy values of 97.2% sensitivity, 80.6% specificity, 83.3% PPV, and 96.7% NPV, while the NycoCard CRP kit produced DA values of 94.4%, 83.3%, 85%, and 93.8% respectively, demonstrating that both kits showed similar performance and provided diagnostically relevant results.

### 2.6.2 Assays for procalcitonin and serum amyloid A

Many assays have been developed to measure PCT, mainly manufactured by BRAHMS. They are briefly summarised in Table 4.

**Table 4. Available assays measuring procalcitonin.**

Assay	Manufacturer	Lower detection limit <sup>‡</sup>	Run time (per measurement)	Sample used	Study used
LUMItest – immunoluminometric assay	BRAHMS	0.5 ng/mL	2.75 hours	20 µl of serum	10, 15, 21, 31, 37, 39, 45, 46, 64
LUMItest*	BRAHMS	0.3 ng/mL	1.5 hours	Serum	84
LIAISON BRAHMS PCT – immunoluminometric assay	DiaSorin	0.1 ng/mL	40 minutes	Serum	25, 35, 84
Kryptor – TRACE assay	BRAHMS	0.06 ng/mL	50 minutes, 19-45 minutes**	Serum	56, 64, 66, 84
PCT kit – ELISA	USCNLIFE	7.8 pg/mL	4.5-5 hours <sup>a</sup>	100 µl of serum or plasma <sup>a</sup>	20
VIDAS –enzyme-linked fluorescent immunoassay	bioMérieux	0.09 ng/mL	20 minutes	Serum	32, 53, 56, 63, 84
PCT-Q –semi-quantitative immunochromatographic kit	BRAHMS	0.5 ng/mL	20-45 minutes	200 µl of serum or plasma	32, 36, 42, 57, 59, 84

Note: \* – revised version; \*\* – subsequent serial measurements; <sup>‡</sup> if functional sensitivity values were not made available, the reported lower detection limits are listed, which may be lower than the functional sensitivity values; <sup>a</sup> – stated on manufacturer’s website.

PCT assay developments have notably improved the functional detection limits and the run times, such as the recently developed Kryptor and VIDAS assays. A recent study reported that the Kryptor and VIDAS systems could be interchangeably used in the clinical setting when using the same cutoff values.<sup>56</sup> Of interesting note is the semi-quantitative PCT-Q kit, made commercially available by BRAHMS as a point-of-care testing (POCT) kit. Results are indicated by one of four different shades of a red coloured band, each of which corresponds to a different range of PCT levels.<sup>42, 57</sup> The ranges indicate the possibility and severity of sepsis. Although the kit is designed to require no specialised training to operate and interpret results, the semi-quantitative nature means that test results are subject to the operating technician’s interpretation.<sup>57</sup> User difficulties in interpreting results have been reported, and its results only showed moderate agreement compared to the Kryptor assay when used in the clinical setting.<sup>57</sup>

Similar to PCT and CRP, multiple assays exist to measure SAA (Table 5).

**Table 5. Available assays measuring serum amyloid A.**

Assay	Manufacturer	Lower detection limit <sup>‡</sup>	Sample used	Study used
BN II analyzer	Dade Behring	68 mg/L	Serum	10, 39
BN ProSpec analyzer	Dade Behring	0.758 mg/L	Serum	23, 48
IMx system	Abbott Laboratories	0.02 mg/L <sup>a</sup>	Serum	40
SAA ELISA kit	BioSource International	1.9 mg/L	Serum	47
LZ TEST “Eiken” SAA kit	Eiken Chemical Co. Ltd	0 mg/L	3 µl of serum	30
N Latex SAA kit	Siemens Healthcare Diagnostics	0.75 mg/L <sup>b</sup>	Serum	43

Note: <sup>‡</sup> if functional sensitivity values were not made available, the reported lower detection limits are listed, which may be lower than the functional sensitivity values; <sup>a</sup> – stated in <sup>85</sup>; <sup>b</sup> – stated in manufacturer’s brochure.

It is interesting to note that the LZ TEST “Eiken” SAA Kit has been cited as a fully automated rapid kit requiring no specialised equipment, with a detection range of 0-386 µg/mL.<sup>30</sup>

### 2.6.3 Assays for mannan and anti-mannan

Assays measuring mannan and anti-mannan concentrations are predominantly made by Bio-Rad Laboratories. These quick tests already exist because cultures for fungal infections are often insensitive and time intensive.<sup>73</sup> These include: the *Platelia Candida*-specific antigen and antibody ELISA kit, with manufacturer suggested cutoff values of 0.5 ng/mL for mannan and 10 AU/mL for anti-mannan;<sup>73</sup> and the *Platelia Aspergillus*-specific antigen immunoassay, with a manufacturer suggested CV of 1.5 ng/mL for mannan.<sup>45</sup> There also appears to be an updated version of the assay kit for the *Candida* species, with manufacturer suggested CVs of 0.25 ng/mL for mannan and 5 AU/mL for anti-mannan.<sup>72</sup> Enzyme immunoassays with greater sensitivities have also been developed.<sup>74</sup>

### 2.6.4 Assays for interferon-γ-inducible protein 10

No quick diagnostic assay for IP-10 are available yet. The assays used in studies utilise different measurement methods, including: a cytometric bead array kit (BD Biosciences Pharmingen) with a lower limit of 2.8 pg/mL, able produce results in 4 hours using 50 µl of plasma;<sup>75</sup> a commercially available sandwich ELISA kit (R&D Systems) with a lower limit of 1.67 pg/mL, able to run on serum;<sup>52</sup> and the Bio-Plex Human 27 Panel (Bio-Rad Laboratories), a multiplex flow cytometry-based assay.<sup>76</sup>

## 2.7 Commentary on sepsis biomarker research

The main challenge facing future biomarker research, and in reviewing biomarker studies, is the lack of standard operating protocols for each specific biomarker. There is high variability in study designs, including small sample sizes,<sup>25, 32, 35-39, 42-46, 48, 63, 76</sup> heterogeneous population types,<sup>31, 32, 35, 46</sup> population type specificity,<sup>25, 36, 38, 45, 46, 63</sup> and high variation in assay equipment. Several studies also suffer from poor presentation and/or application of statistical analysis of data,<sup>10, 25, 31, 32, 35-37, 39, 40, 42-45, 48, 53, 63</sup> which may lead to improper interpretation of results by the readers. Many studies are single-centre studies involving small sample sizes, which may result in incorrect representation of the general population, but this restriction is a result of the high costs of running studies in the clinical setting and incorporating multiple centres. However, other issues pertaining to study design requires the establishment of standardisation among biomarker research studies.<sup>21, 58, 62</sup> Efforts have already been made to establish reporting and analysis standards, such as STARD<sup>86, 87</sup> and GRADE<sup>88, 89</sup> respectively, and the research community should endeavour to adopt these standards on a global scale for all future studies.

Although CRP and PCT are both commonly studied biomarkers for sepsis and infection, some studies suggest neither can be used in singular capacities. CRP shows a 12-24 hour delay in elevated levels to infection,<sup>20, 58</sup> so it may not be a sensitive marker during initial measurement.<sup>75</sup> Serum PCT levels can naturally rise 3-24 hours after exercise.<sup>58</sup> In newborn infants, PCT also naturally increases to 2-3 ng/mL at 24 hours after birth, returning to normal levels at 48-72 hours after birth.<sup>54</sup> A few non-infectious diseases and conditions can also cause abnormally elevated levels of CRP<sup>10, 19, 41, 80</sup> or PCT.<sup>21, 30, 58</sup> In addition, some studies report CRP<sup>30, 32, 35, 39, 42, 46, 75, 83</sup> and PCT<sup>15, 20, 27, 31, 35</sup> to be less diagnostically relevant than other potential biomarkers of sepsis. The current research suggests that a singular “ideal” biomarker of perfect diagnostic relevance and accuracy does not yet exist.<sup>19</sup> However, the many studies reporting the usefulness of CRP, PCT, and other molecules as biomarkers of sepsis cannot be ignored. To overcome this issue, multiple biomarkers must be used in combination to provide definitive diagnostic test results.

A possible strategy is described in Figure 1. Many of the studies reviewed have also demonstrated the use and/or need of measuring multiple markers in combination,<sup>10, 21, 31, 35, 40, 45, 53, 64, 65, 72, 73</sup> generally reporting improved DA values. POCT kit developers are also calling for the development of multiplex assays for various diseases,<sup>2-4, 90</sup> emphasising the need and benefits of multiplex POCT kits.

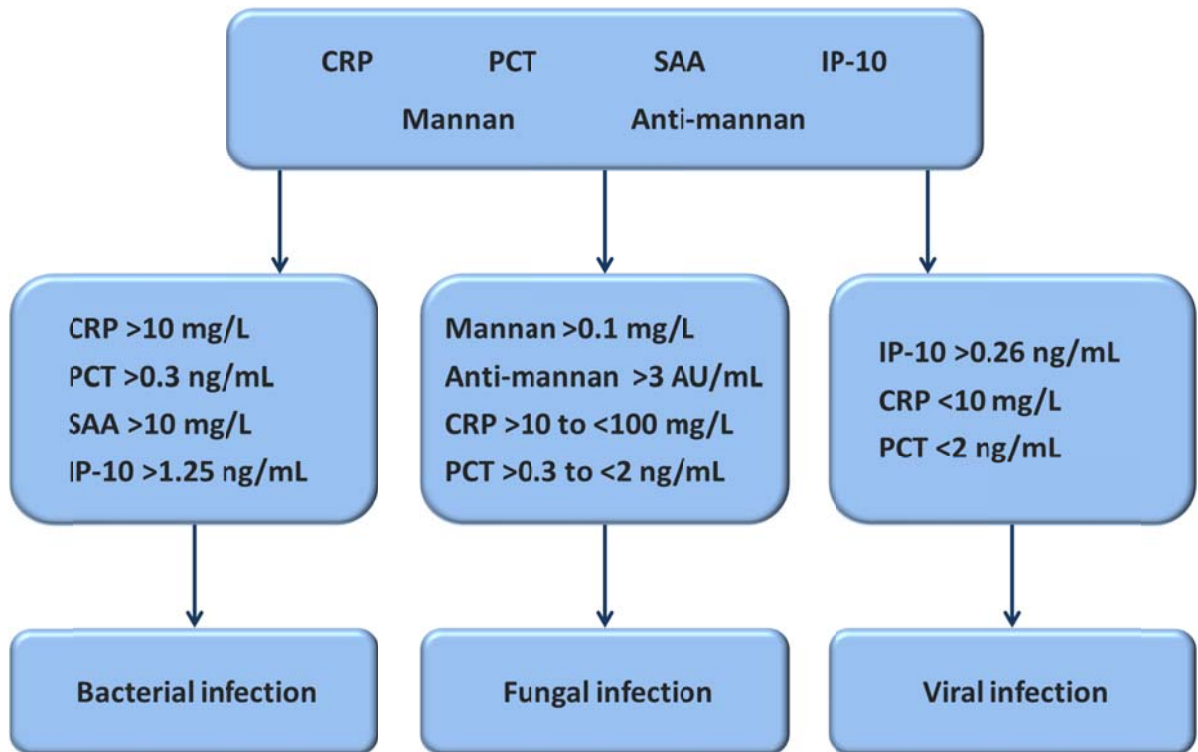


**Figure 1. A possible strategy for diagnosing the type of infectious cause of sepsis.** CRP – C-reactive protein; IP-10 - interferon- $\gamma$ -inducible protein; PCT – procalcitonin, SAA – serum amyloid A.

Further study of POCT kits for sepsis, specifically able to distinguish between bacterial, fungal, and viral infectious causes, would provide substantial benefit in patient care, compared to already available diagnostic assays. There are two main benefits. Firstly, knowing the type of infectious causes of sepsis would prevent broad antimicrobial use, thereby reducing occurrences of drug toxicity and drug-resistant microbes, and ultimately resulting in greater patient comfort. Secondly, identifying the type of infectious cause would allow earlier use of specialised cultures and diagnostic tests specific to bacteria, fungi, or viruses, leading to diagnostic results of greater sensitivity.

## 2.8 Five year outlook

Although recent advances in molecular biology and biochemistry will lead to the discovery of new biomarkers for sepsis, the bottleneck challenge in the diagnosis of sepsis remains determining the diagnostic relevancy of biomarkers with absolute certainty. The keys to verifying their diagnostic

relevancies are standardisation in study methodology and use of assays with better detection limits. Assays capable of lower functional detection limits should be readily available for these purposes as several are already in development, while new technologies will allow improvements to existing ones. The ongoing development of POCT kits for other diseases may also be beneficial for sepsis biomarker research. Designs from these kits can be applied towards developing a sepsis diagnostic kit that may ultimately provide greater accuracy and faster results over current assays. The standardisation of study methodology is a complicated task and may not occur within the next five years. Researchers should seize the opportunity at current annual conferences on sepsis and biomarker research to achieve some consensus on methodology standards.

In parallel, general consensus in the scientific community regarding the diagnostic relevancies of the current sepsis biomarkers needs to be established within the next few years. Consequently, the direction of research will need to evolve from single-centre to multi-centre studies to reduce the limitation of generalisation of small data sets. Sepsis often presents alongside other conditions. Due to this complexity, a single “golden” biomarker may not exist, thus research should shift more focus on assessing the combined diagnostic capabilities of multiple biomarkers.

Complementary research paths also exist and should be explored. Firstly, as sepsis results from systemic infection, the most diagnostically relevant sepsis biomarkers should be studied for their potential towards early diagnosis of general infections. Results from these studies can be applied to the development of POCT kits designed to monitor sudden homeostatic imbalances, indicating the body is diseased before symptoms are presented. Secondly, some research should be devoted to designing and testing a rigorous, multiplex POCT kit for sepsis within the next five years, which would be beneficial for both method standardisation in future research and clinical usage in rural and low income communities.

### **3.0 Research objectives**

This thesis focuses on the development of a colorimetric, magnetically separable sensor for the capture and detection of biomarkers, based on a surface-functionalised core-shell particle design. Delivering a colorimetric response to biomolecule detection was desired in order to produce an easily identifiable sensing signal that could be observed without specialised laboratory equipment. To accomplish this objective, a sensing system capable of amplifying the detection of small protein concentrations was required. Magnetic separability was also desired because it would offer two main benefits. First, it would allow the design of a solution-based sensor, advantageous over solid-state systems because of the increased probability of interactions between sensor and analyte, as well as allowing biomolecule-based analytes to preserve their native form and function.<sup>91</sup> Second, magnetic separability would achieve simple, rapid separation of captured targets from complex solutions, thereby allowing the sensor to be used with non-manipulated samples such as human blood. These properties were chosen to adhere to the guidelines of point-care-testing devices previously elucidated, so that the sensor can act as a POCT platform for sepsis and other possible diagnostic applications. This thesis discusses the steps taken to develop, demonstrate and tune the sensor properties.

#### **3.1 Sensor development for biomolecule detection objectives**

Various materials were considered to achieve a colorimetric sensing platform. The ideal material had to demonstrate a distinct range of colours to stimuli that was easily distinguishable to the naked eye, and possess functional groups for conjugation to receptor components. Polydiacetylenes (PDAs), a class of conjugated polymers possessing unique optical properties,<sup>91</sup> fulfilled these requirements and were previously demonstrated to detect biomolecule in various sensing platforms.<sup>92</sup> The alternating ene-yne polymer backbone structure of PDAs allows them to absorb multiple photons<sup>93</sup> and express a dark blue colour when the diacetylene monomers undergo photoinduced topopolymerisation.<sup>94</sup> External stimuli to the polymer backbone,<sup>95</sup> such as the surface pressure caused by receptor-ligand interactions at the polymer surface, have been demonstrated to cause the polymer to display a colour transition progressing through a gradient of colours from blue to purple to bright red.<sup>96-98</sup> The colour transition can be quickly analysed with absorbance spectrophotometry for quantitative evaluation.<sup>99</sup> In addition, the diacetylene monomers are composed of a hydrocarbon chain with a single carboxyl group at one end, ideal for directed conjugation to other materials. For example, a commercially available diacetylene monomer was previously conjugated to polar

compounds to improve its amphiphilic properties,<sup>100</sup> or to various ligands such as antibodies and enzymes for detection of target molecules.<sup>92</sup>

Previous PDA sensors have commonly employed solid-state approaches such as silica-supported<sup>101</sup> and glass-supported<sup>99, 102</sup> thin films, while solution-based sensors have utilised liposome structures.<sup>103, 104</sup> The problem with the existing solution-based approach is that only purified, single target samples can be used, and separation of liposomes from solution is not possible without specialised equipment. To address this, a new solution-based platform has been developed where amphiphilic PDA is used to coat superparamagnetic iron oxide nanoparticles (SPIONs) to form colorimetric, magnetically separable sensors. SPIONs were chosen as the ideal magnetic materials because they are easily synthesised, demonstrate magnetism only when an external magnetic field is applied, achieve similar activity as ferromagnetic materials, and retain negligible residual magnetism when the field is removed.<sup>105-107</sup> Bovine serum albumin (BSA), a cheap, commonly available serum protein, is used to functionalise the sensor surface. The functionalised sensors are used to detect anti-BSA antibodies in native antiserum solution in order to demonstrate its colorimetric and magnetic separation properties. This work is significant as it introduces a new sensing platform for potential use in POCT applications, capable of capturing and detecting biomolecules.

Specific objectives for this work have been:

1. Synthesis of amphiphilic diacetylene monomers.
2. Synthesis of PDA-coated SPIONs.
3. Visual and spectroscopic evaluation of colour responsiveness and magnetic separability.
4. Demonstration of capture and colorimetric detection of a biomolecule from a complex solution.

### **3.2 Sensor tuning objectives**

Following the development and demonstration of biosensor performance, optimisation of the sensor was required. A proposed theory in earlier work was that colour responsiveness could be tuned by varying the amount of PDA, since it should be expected that higher concentrations of PDA will provide a larger percentage of crosslinked networks.<sup>98</sup> Improving the lower detection limit was also critically important, especially for the detection of biomarkers such as C-reactive protein, where serum concentrations above 0.01 mg/mL are indicative of sepsis.<sup>41</sup> This work describes the optimisation of coating amphiphilic PDA on SPIONs and tuning of the colorimetric and magnetic

separation properties, leading to an improved lower detection limit than previously reported. Tuning the colour response is achieved by varying the weight percent ratio of amphiphilic PDA to SPIONs during fabrication while keeping the amount of SPIONs constant. Optimisation is demonstrated by surface functionalisation with antibodies, compared to the previously demonstrated sensor utilising bovine serum albumin, additionally demonstrating the versatility of the biosensor for the detection of other biomarkers and materials.

Specific objectives for this work have been:

1. Tuning the colorimetric response by varying the PDA concentration used in sensor fabrication.
2. Evaluation of varying PDA concentrations on magnetic separability.
3. Determination of the optimal PDA to SPION ratio for sensor fabrication.
4. Demonstration of sensor's versatility for biomolecule detection by functionalisation with antibodies.
5. Improvement of the sensor's lower detection limit.

## **4.0 Development of a Colorimetric, Superparamagnetic Biosensor for the Capture and Detection of Biomolecules**

### **4.1 Introduction**

This section of the thesis describes the development of the surface-functionalizable core-shell particle biosensor composed of a superparamagnetic iron oxide nanoparticle (SPION) core and an amphiphilic polydiacetylene (PDA) shell, capable of measurable colorimetric sensing and simple, rapid magnetic separation for the capture and detection of biomarkers (Figure 2). The diacetylene monomer 10,12-pentacosadiynoic acid was chosen because of its chemical structure, and previous demonstrations of its ability to form protein sensing<sup>108</sup> to optical detection of foodborne pathogens.<sup>99, 109</sup> SPION was chosen because of their simple synthesis and superparamagnetic properties, allowing for simple and rapid magnetic separation of captured biomolecules. Nanoprecipitation was used to fabricate the sensors, which appear as macroscopic particles that are easily visualised with the naked eye. The sensors were functionalised with bovine serum albumin (BSA) to detect and capture anti-BSA antibodies from a complex antiserum solution. This sensor is significant because it is the first to combine PDA and SPIONs to form a colorimetric, magnetically separable biosensor, and is demonstrated to successfully detect and capture a target biomolecule from a complex biological solution.

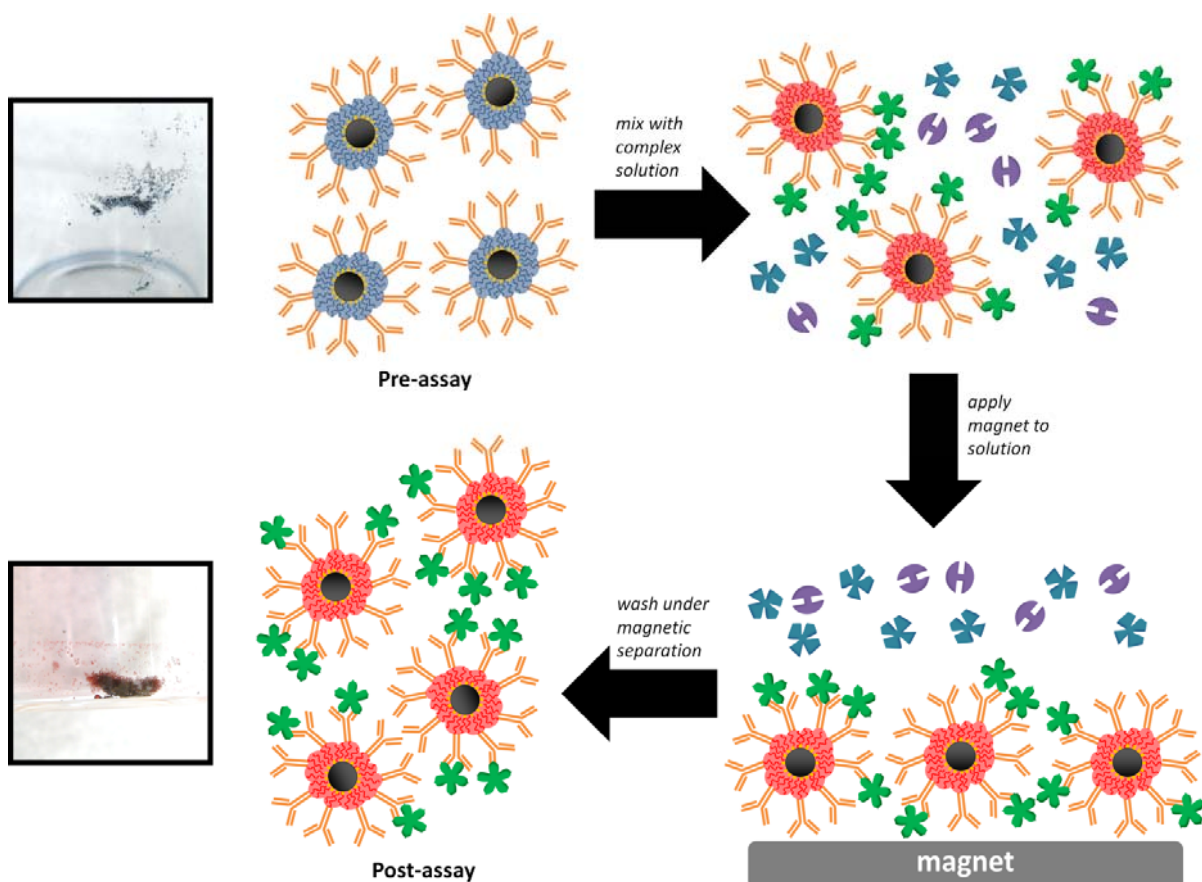


**Figure 2. Schematic representation of colorimetric, magnetically separable functionalised Lys-PCDA/SPIION particles, describing the capturing and sensing of a target biomolecule from a complex solution.** On the left are photographs of actual magnetically separated Lys-PCDA/SPIONs before and after the detection of ethanol.

## 4.2 Experimental Methods

### 4.2.1 Synthesis of hydrophobic superparamagnetic iron oxide nanoparticles

Oleic acid-coated SPIONs (OA-SPIONs) were synthesised according to a previously described coprecipitation method, with minor modifications.<sup>110</sup> Briefly, excess oleic acid was used to promote a uniform coating on the SPIONs, while undecylenic acid was not used. The OA-SPIONs were characterised using a Philips CM10 transmission electron microscope. The hydrophobic coating was verified by dispersing the OA-SPIONs in a chloroform/water mixture (see Appendix A).

#### **4.2.2 Amphiphilic modification of diacetylene monomer**

The diacetylene monomer 10,12-pentacosadiynoic acid (PCDA) (Alfa Aesar) was modified with a hydrophilic lysine derivative, *N*<sub>α</sub>,*N*<sub>α</sub>-bis(carboxymethyl)-L-lysine hydrate (BCML) (Sigma Aldrich) via two-step coupling chemistry using 1-ethyl-3-(3-dimethylaminopropyl) carbodiimide (EDC) and N-hydroxysuccinimide (NHS) (see Appendix A). The NHS-activated PCDA was reacted with a 1.2 molar excess of BCML, precipitated and washed with 1 M hydrochloric acid, extracted with chloroform/ethanol (1:1), then filtered and dried to obtain a purplish white paste. To confirm the synthesis of the lysine-modified PCDA (Lys-PCDA), the product was characterised using <sup>1</sup>H nuclear magnetic resonance spectroscopy (Bruker Avance 300MHz).

#### **4.2.3 Fabrication of Lys-PCDA/SPION core-shell particle**

To prepare the Lys-PCDA/SPION particles, the OA-SPIONs and Lys-PCDA were mixed together in tetrahydrofuran. Self-assembly of Lys-PCDA onto OA-SPIONs was achieved through dropwise addition of the mixture into Milli-Q water under constant stirring. The particles were washed several times with water, then irradiated at 254 nm with a UV crosslinker (UVP CL-1000), causing polymerisation of the Lys-PCDA surface coating. This was marked by a visible colour change of the particles from brown to a black to dark blue colour, depending on the percent concentration of Lys-PCDA added.

#### **4.2.4 Detection of anti-bovine serum albumin antibodies**

Particles used for the detection of anti-BSA antibodies were synthesised as before, excluding UV irradiation. To functionalise the particle surface with BSA, they were activated with EDC and N-hydroxysulfosuccinimide (sulfo-NHS) in a 0.1 M MES buffer, pH 4.7, and washed, repeated twice, then mixed end-over-end with 20 mg/mL BSA in sterile 0.1 M PBS buffer, pH 7.2, overnight at 4°C. The particles were washed to remove unconjugated BSA and mixed with 40 mM ethanolamine in water, pH 8.3, to block unreacted sulfo-NHS sites. The particles were washed several times again, then the Lys-PCDA coating was crosslinked at 254 nm in 10 bursts of 1 mJ/cm<sup>2</sup>. All washes were performed with PBS buffer, using a magnet to separate the particles from the decanted solution.

The assay was performed by incubating approximately 1.25 mg/mL of BSA/Lys-PCDA/SPION particles in 1 mL aliquots of various concentrations of rabbit anti-BSA antiserum, of which anti-BSA polyclonal antibodies formed a ~10% fraction of the antiserum proteins according to

manufacturer's specifications (Rockland Immunochemicals Inc.). The particles were continuously mixed with a low speed vortex mixer overnight, then washed several times with PBS buffer using magnetic separation. The particle color transition was measured with a BioTek Epoch UV-visible spectrophotometer in the visible absorbance spectrum.

The colour transition was quantified as a colorimetric response (CR %), using the following:<sup>111</sup>

$$CR \% = \frac{(PB_0 - PB_1)}{PB_0} \times 100\%$$

where  $PB = A_{blue}/(A_{blue} + A_{red})$ ,  $A$  was the UV-visible absorbance value of the particle's "blue" state at 650 nm or the "red" state at 550 nm, and  $PB_0$  and  $PB_1$  were the respective colorimetric ratios of the particles before and after the assay.

## 4.3 Results and Discussion

### 4.3.1 Characterisation of Lys-PCDA/SPION-based biosensors

The objective in this study was to develop a magnetically separable sensor capable of displaying a distinct colorimetric response to receptor-ligand interactions, and thus suitable for POCT sensing applications. By incorporating a hydrophilic lysine derivative, the Lys-PCDA/SPIONs display sustained suspension in aqueous solutions compared to particles formed with unmodified PCDA (Figure 3(A-B)), essential for maximising particle interaction with aqueous soluble analytes such as serum proteins. To confirm the colour functionality of the sensor, the particles were added to ethanol, resulting in a sharp colour transition from a blue to a red state, similar to previously described PCDA vesicles.<sup>99, 108, 112</sup> This also resulted in an absorbance peak shift from 650 nm to 550 nm (Figure 1(C-E)). Ethanol has been previously reported to cause PDA vesicles to change from blue to red, due to swelling of the PDA layers as ethanol interacts with the PDA carboxyl group through hydrogen bonding.<sup>112</sup> Applying a magnetic field to the particles in solution resulted in quick particle separation without causing changes in colour. In addition, the particles remained magnetically separable after undergoing the colour transition. This was marked by the solution becoming clear and colourless and was easily observed with the naked eye due to the particle size (Figure 3(D)), illustrating the successful capture of particles after a sensing event. In rapid diagnostic applications involving complex or non-manipulated fluids, the ability to quickly and easily separate analytes for analysis without adversely affecting the sensor is a necessary functionality, which the sensor particles demonstrated through this initial performance characterisation.

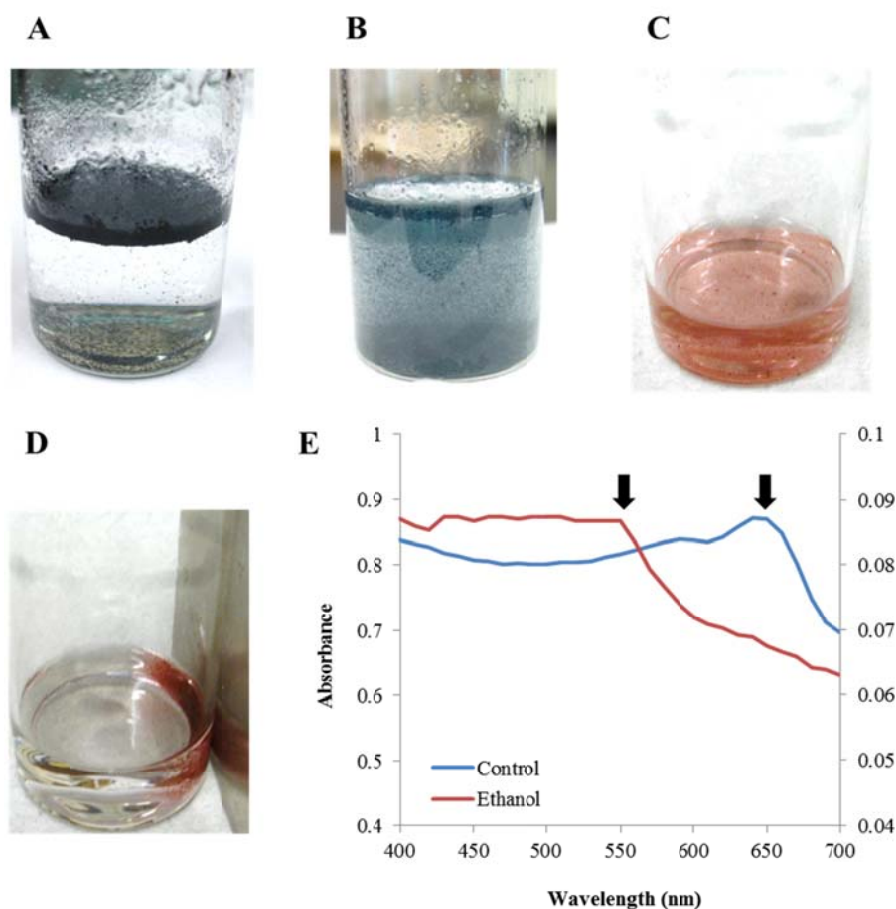


**Figure 3. Demonstration of the colorimetric and magnetic properties of Lys-PCDA/SPIONs.** (A) PCDA/SPIONs in water, (B) Lys-PCDA/SPIONs in water, (C) in ethanol, (D) while applying a magnet, and (E) visible absorbance spectra before and after addition of ethanol. The increase at 550 nm and decrease at 650nm marked with black arrows correspond to the colour transition.

#### 4.3.2 Colorimetric performance of Lys-PCDA/SPION sensors

Biosensors developed for POCT applications must meet several criteria,<sup>2</sup> including: yielding easily interpretable results, requiring little to no sample manipulation, and requiring no specialised training or equipment to operate. Many serum proteins of interest are commonly present at low concentrations, requiring signal amplification of the detection event, such as a colorimetric response. To generate easily interpretable, equipment-free results, it is critically important that the detection of specific concentrations or concentration ranges correspond to distinguishable colors or color

gradients. In this study, one objective was to demonstrate the suitability of the Lys-PCDA/SPIONs for POCT applications by demonstrating the detection of receptor-ligand interactions, using BSA-functionalised sensors to detect anti-BSA antibodies. The functionalised particles exhibit a visible, increasing colorimetric response as the concentration of anti-BSA are increased, ranging from a blackish blue colour to a gradient of increasingly lighter purples (Figure 4(A)).

The use of anti-BSA in antiserum format highlights the importance of magnetic separability for analyte capture and detection, especially for POCT applications. As shown in Figure 4(A-II), the purified antiserum appears as a clear reddish yellow solution, which hinders accurate judgment the degree of colour response with the naked eye at the end of the assay. Based on current results and previous studies of PDA-based sensors,<sup>109</sup> PDAs are known to exhibit a colour response ranging from dark purple to bright red in response to stimuli. It can be safely inferred that PDA-based sensors used with non-manipulated blood or other dark coloured samples would mask any colour transitions and make accurate interpretations of the results with the naked eye very difficult. As a result of the SPION cores, the particles demonstrated quick separation from solution with a common magnet, avoiding the need for specialised equipment to wash and observe the particles, and allowing accurate observation of the increased expression of purple among the different samples (Figure 4(A-III)). Based on the visual observations alone, Lys-PCDA/SPION particles can serve as a platform for the colorimetric detection and capture of analytes from solution, both ideal properties for POCT applications.

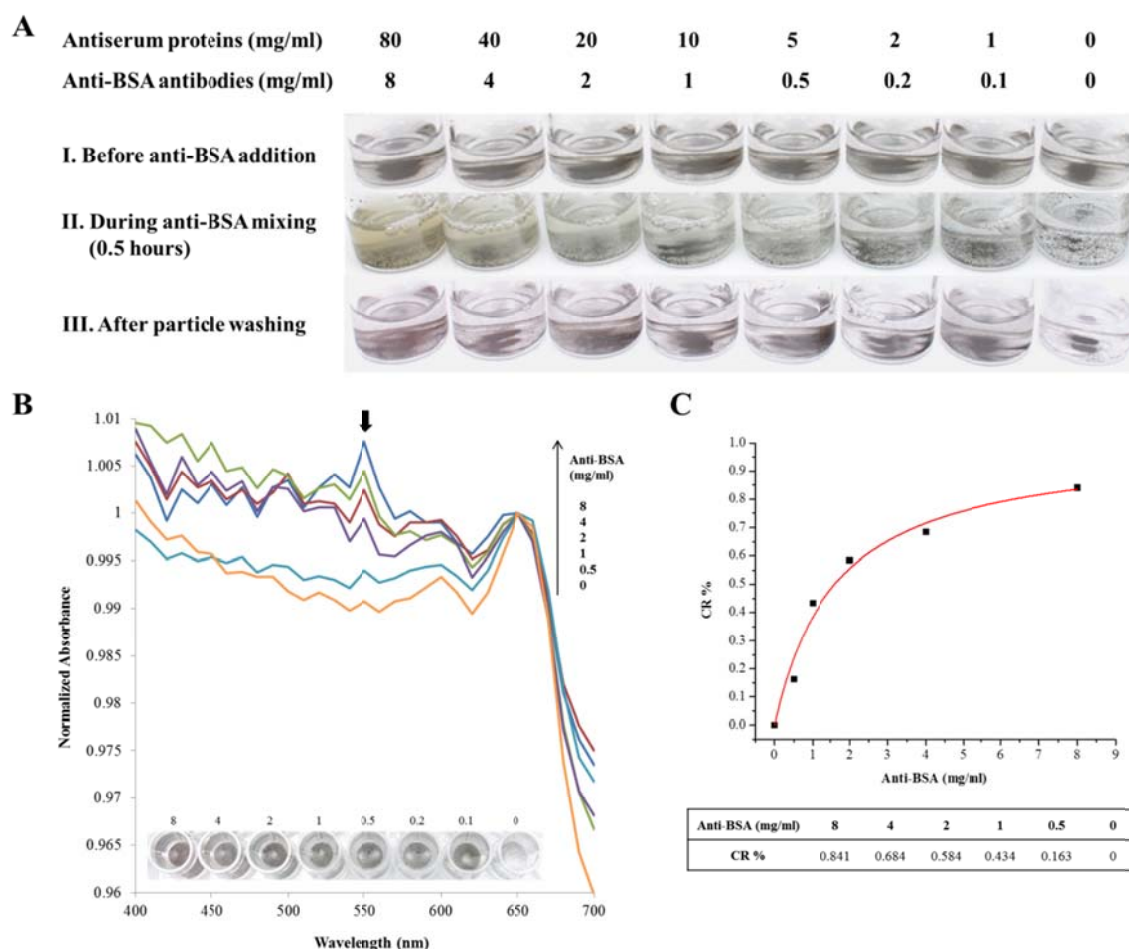


**Figure 4. Biosensor performance of BSA-functionalised Lys-PCDA/SPIONs.** (A) Particles before, during, and after incubation in anti-BSA antiserum. (B) Comparison of colorimetric response after detection of anti-BSA. Responses are measured at the “red” state peak at 550 nm, indicated by the bolded black arrow. Overlaid is a photograph of a subsection of the 96-well microplate used, labeled with the anti-BSA concentrations. (C) Regression analysis of the colorimetric response values.

To verify the accuracy of the visual observations and illustrate the analytical performance of Lys-PCDA/SPION sensors, the visible absorbance spectra of the samples were measured and normalised against the “blue” state peak at 650 nm. The absorbance at 550 nm (the “red” state), which is used to calculate the degree of colour change for PDA-based sensors, showed an increasing trend as the concentration of anti-BSA was increased (Figure 4(B)). Similar trends of increasing “red” state absorbance values in response to increasing analyte concentrations have previously been

reported, including in the detection of *S. typhimurium* cultures<sup>99</sup> and amino acids.<sup>108</sup> Quantitative analysis, expressed as CR %, described an increasing colorimetric response of 0.163, 0.434, 0.584, 0.684, and 0.841% for samples with 0.5, 1, 2, 4, and 8 mg/mL anti-BSA, respectively, compared to particles from the 0 mg/mL anti-BSA sample (Figure 4(C)). In comparison, when the particles were added to ethanol, a maximum CR % of only 1.796% was achieved, indicating that approximately half of the possible colour response range was achieved. For diagnostic applications interested in 0-10 mg/mL of analyte, it is expected the sensor particles could express the entire colour response range by optimising the ratio of Lys-PCDA to SPIONs and achieve greater colour distinctions between differing amounts of analyte. The colorimetric response values showed a hyperbolic regression with a coefficient of determination of 0.9806 (see Appendix A), indicating that if larger amounts of anti-BSA had been tested with the Lys-PCDA/SPIONs, the full colour response range would have likely been realised. The results also demonstrate that the Lys-PCDA/SPIONs can be used as analytical biosensors in addition to semi-quantitative POCT applications.

#### **4.4 Conclusions**

The simple synthesis and application of novel Lys-PCDA/SPION particles as a platform for the capture and detection of serum proteins was demonstrated in this study. Although only a proof-of-concept investigation was performed, the biosensor showed a colorimetric response that corresponded to an increasing concentration of anti-BSA antibodies, with a lower detection limit of 0.5 mg/mL. Thus, in its current form, the biosensor would be useful for diagnostic applications where high biomarker concentrations are indicative of disease, as well as non-clinical applications where analyte detection is needed in the mg/mL range. Additionally, the colorimetric response was both easily visualised with the naked eye and could be measured with a basic UV-Vis spectrophotometer. The response could be accurately measured because the particles could be quickly separated from a mixed solution with a common magnet, eliminating the need for advanced equipment such as high-speed centrifuges or laborious wash techniques. Future studies are needed to improve the sensing performance of the particles and achieve a greater range of colorimetric response, including increasing the Lys-PCDA to SPION ratio. This work has demonstrated that Lys-PCDA/SPION particles can be quickly developed for clinical applications and address a pressing need for POCT platforms.

## 5.0 Optimisation of polydiacetylene-coated superparamagnetic iron oxide for colorimetric detection and capture of biomarkers

### 5.1 Introduction

This section of the thesis describes the optimisation of the polydiacetylene-coated SPION biosensor for capturing and detection biomarkers, previously described in section 4.0. To tune the colorimetric response of the biosensors, various ratios of Lys-PCDA to SPION were tested during biosensor fabrication while keeping the SPION content constant in all compositions. Varying the maximum colour response of each composition was achieved by exposing the sensors to ethanol. Colorimetric detection was achieved by functionalising the sensors with anti-horse IgG antibody and incubating the sensors against purified horse IgG solution. Similar to previous studies of PDA-based sensors, characterisation of each sensor composition was performed with UV-visible absorption spectrophotometry. The work is significant because it resulted in determining the optimal ratio of Lys-PCDA to SPION to achieve the maximum sensor performance, including colorimetric response and magnetic separability. The lower detection limit was also improved to a significant biomarker concentration, equal to C-reactive protein levels used for diagnosing sepsis. It also demonstrates the versatility of the biosensor as a different receptor-ligand system is used in this work to express the colorimetric response.

### 5.2 Experimental Methods

#### 5.2.1 Materials

10,12-Pentacosadiynoic acid (PCDA) was purchased from Alfa Aesar and purified with 0.45  $\mu\text{m}$  polytetrafluoroethylene membrane filter before use. (*S*)-*N*-(5-Amino-1-carboxypentyl)iminodiacetic acid, *cis*-9-octadecenoic acid, 1-ethyl-3-(3-dimethylaminopropyl) carbodiimide (EDC), 1-hydroxy-2,5-pyrrolidinedione, hydroxy-2,5-dioxopyrrolidine-3-sulfonic acid sodium salt (sulfo-NHS), and 2-aminoethanol purchased from Sigma Aldrich (Canada), NaCl, FeCl<sub>2</sub>, and Fe<sub>2</sub>(SO<sub>4</sub>)<sub>3</sub> purchased from Fisher Scientific (Canada), and *N,N*-diethylethanamine, NH<sub>4</sub>OH, HCl, CHCl<sub>3</sub>, tetrahydrofuran (THF), and ethanol purchased from EMD Millipore were used as received. All solvents used were HPLC grade. Horse IgG and rabbit anti-horse IgG antibodies were purchased from Rockland Immunochemicals Inc. and washed with sterile PBS buffer (0.1M sodium phosphate,

0.15M NaCl, pH 7.2) using Amicon Ultra-15 10K centrifugal filter units from EMD Millipore before use.

### **5.2.2 Synthesis**

Oleic acid-coated SPIONs (OA-SPIONs) and amphiphilic PDA (Lys-PCDA) were synthesised using procedures as previously described in section 4.2.

### **5.2.3 Biosensor fabrication**

Functionalised amphiphilic PDA-coated SPION sensors (Lys-PCDA/SPIONs) were fabricated at various weight percentages (wt%) of Lys-PCDA ranging from 60-95 wt% while keeping constant the amount of OA-SPIONs, similar to the previously described procedure in section 4.2. Briefly, Lys-PCDA and OA-SPIONs were mixed in THF and added dropwise to Milli-Q water at 12 mL/h under mechanical stirring at 820 rpm, stirred for 20 minutes, then washed using magnetic separation. Sensors were functionalised with equal amounts of anti-horse IgG antibody according to the molar fraction of Lys-PCDA in each wt% sample, via two-step EDC/sulfo-NHS conjugation in PBS buffer. Unreacted sulfo-NHS was blocked with 2-aminoethanol. Fabrication was completed with irradiation at 254 nm in 3 bursts of 1 mJ/cm<sup>2</sup>.

### **5.2.4 Antibody assay**

Equal aliquots of each wt% sample of Lys-PCDA/SPIONs were incubated with 4 mL of 0, 0.01, 0.1, 0.5, and 1 mg/mL horse IgG in PBS buffer and mixed at room temperature with gentle orbital shaking until marked colour changes were observed (6 hours).

### **5.2.5 Characterisation**

The antibody assay was monitored at set time intervals for the appearance of colour change and photographed at each interval in a controlled white-surfaced digital photo box with identical lighting and camera settings. UV-visible absorption measurements were recorded at the end of the antibody incubation with a Biotek Epoch spectrophotometer using Greiner Bio-One UV-Star 96-well microplates. Lys-PCDA/SPIONs were washed 3 times with PBS buffer before spectroscopic analysis to remove any interference effects from the horse IgG solution. Spectra with a wavelength range of 400 to 700 nm, in 10 nm increments, were recorded. The color transition was quantified as a colorimetric response (CR %), using the following:<sup>111</sup>

$$CR \% = \frac{(PB_0 - PB_1)}{PB_0} \times 100\%$$

where  $PB = A_{blue}/(A_{blue} + A_{red})$ ,  $A$  was the UV-visible absorbance value of the particle's "blue" state at 650 nm or the "red" state at 540 nm, and  $PB_0$  and  $PB_1$  were the respective colorimetric ratios of the particles before and after the assay.

## 5.3 Results and discussion

### 5.3.1 Optimisation of polydiacetylene amount used in sensor fabrication

The objective of this work was to optimise and tune the colorimetric performance of previously described Lys-PCDA/SPION sensors by varying the ratio of amphiphilic PDA to hydrophobic SPIONs during sensor fabrication. Normalised absorption spectra and visual comparisons of the sensors not used in the assay are shown in Figure 5 and clearly demonstrate the effects of increasing the amount of PDA, which are three-fold. First, increasing the amount of PDA results in distinct increases in the initial blue colour, as well as a greater colour response when perturbed with ethanol (Figure 5(A-C)), which has been previously reported to swell PDA surfaces and affect a transition to the "red" state.<sup>112</sup> For example, sensors composed of 95 wt% PDA demonstrated a 23.054% colorimetric response compared to a 0.678% response from 60 wt% PDA sensors (Figure 5(D)).

Second, increasing the amount of PDA assists in shielding the UV-visible absorption interference caused by the black SPION cores, up to 90 wt% PDA, indicated by the absorbance values between 400-600 nm. Previous free-floating PDA vesicles have demonstrated decreasing absorption values from ~590 nm to 400 nm.<sup>98</sup> In comparison, the Lys-PCDA/SPIONs do not display this trend. At lower PDA wt%, markedly noticeable among 60-75 wt%, the PDA surface coating is not thick enough to reduce absorption by the SPION core. However, it is important to note that this interference does not affect the "red" state reading at 540 nm if enough PDA is used during fabrication, indicated by the marked peaks at 540 nm among the 75-95 wt% PDA sensors (Figure 5(C)).

Third, increasing the amount of PDA greatly improves the aqueous dispersion of the Lys-PCDA/SPION sensors. This is visually demonstrated by the denser solutions at higher PDA wt%, in comparison to the increasingly clear solutions at 70-60 wt% PDA (Figure 5(A)). During wash steps of biosensor fabrication, the lower wt% sensor particles were observed to preferentially float at the

surface of the aqueous solutions. This prevented efficient magnetic separation and retention of the Lys-PCDA/SPIONs, resulting in the loss of sensor particles. However, high wt% was also observed to be undesirable, specifically at 95 and 90 wt% PDA. During wash steps, these sensors required longer separation times, and a small fraction of these sensor particles were observed in wash run-off, particularly the 95 wt% Lys-PCDA/SPIONs. In addition to reducing the absorption interference caused by the SPION cores, it is highly suspected the thicker PDA coatings also reduced the net saturation magnetisation of the SPION cores, and thus lowering their magnetic separability. It has been previously shown that magnetic separation of SPIONs is dependent upon the concentration and aggregation of the magnetic material in the net system.<sup>113, 114</sup> Thus, increasing the amount of non-magnetic material between SPIONs, such as found in the high wt% PDA sensors, would be expected to interfere with the transient aggregation of neighbouring SPIONs that allows their separation to occur. This observation coincides with a previous study which found that increasing the amount of non-magnetic material in relation to the amount of hydrophobic SPIONs present in the system resulted in decreasing net saturation magnetisation,<sup>110</sup> which would be expected to reduce their separability.

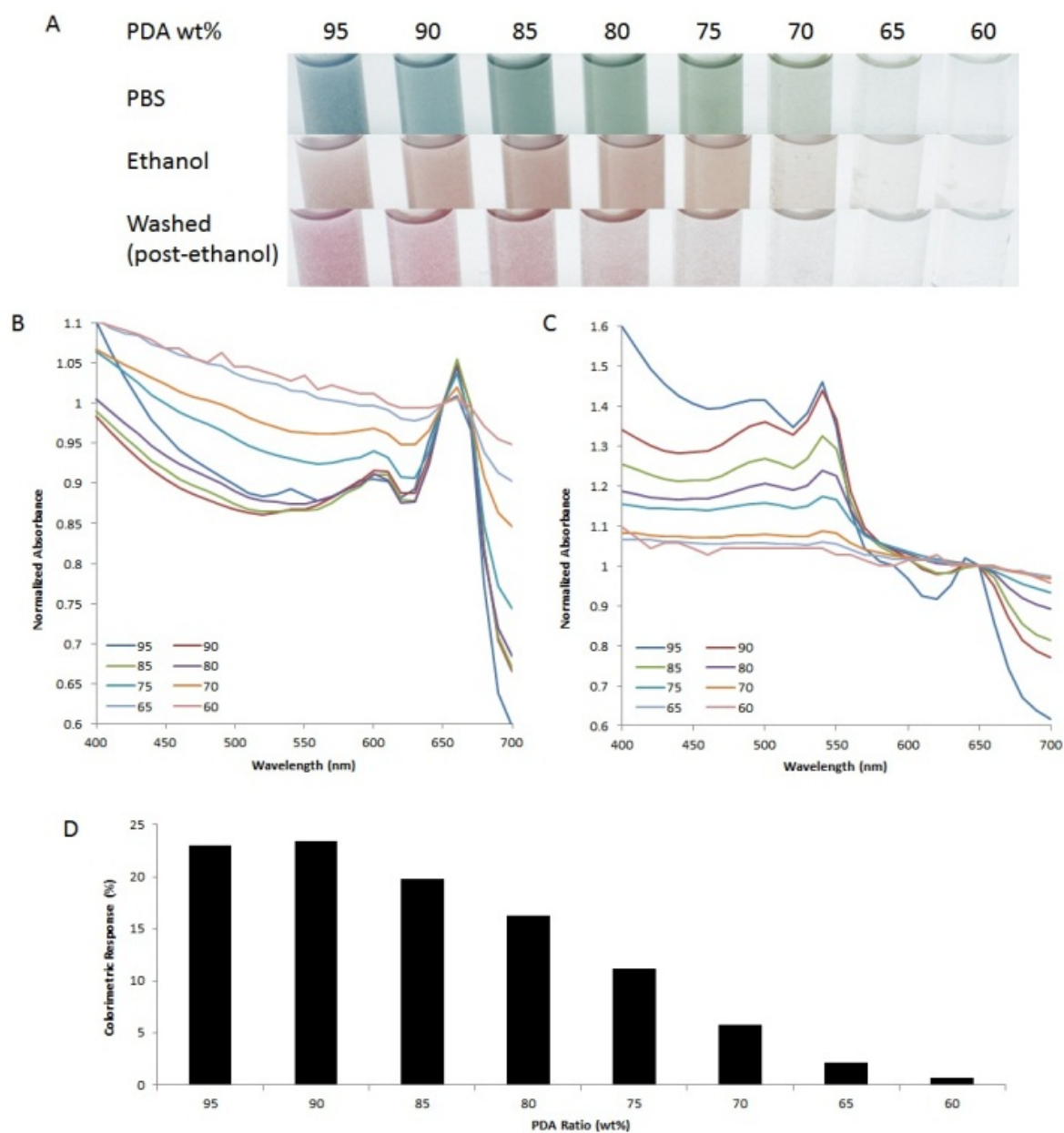


**Figure 5. Characterisation of Lys-PCDA/SPION sensors.** (A) Photographs of varying PDA wt% sensors. (B) Absorption spectra in PBS. (C) Absorption spectra post-ethanol. (D) Colorimetric response of sensors to ethanol.

### 5.3.2 Optimisation of colorimetric biomolecule detection

To optimise the colorimetric detection, each sensor composition was exposed to varying concentrations of horse IgG solution. As shown in Figure 6, the sensors composed of 85-95 wt% PDA demonstrated the most noticeable colour transitions in all four concentrations tested (0.01, 0.1, 0.5, and 1 mg/mL), making a visible transition towards the red state and appearing as the purple colour phase after 6 hours. Similar to previous visual observations when tested against ethanol, increasing the wt% of PDA in the sensor resulted in a greater colour response to biomolecule detection. However, after washing the sensors for spectrophotometry analysis, 90 and 95 wt% sensors showed marked reductions in sensor particle retention, with 95 wt% sensors exhibiting less retention than 90 wt%. This is consistent with earlier observations noted above and indicates that utilising too much PDA can result in suboptimal magnetic separability.

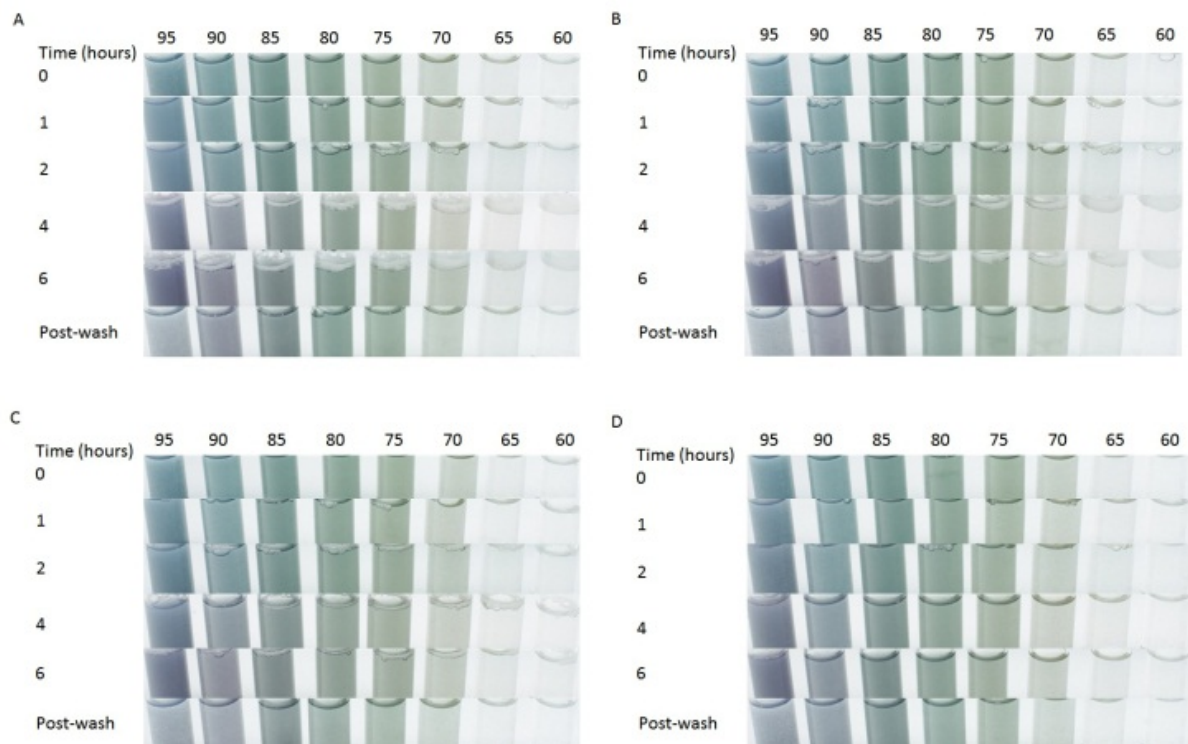


**Figure 6. Photographs of Lys-PCDA/SPION sensors of varying PDA wt%. (A) 1 mg/mL horse IgG. (B) 0.5 mg/mL horse IgG. (C) 0.1 mg/mL horse IgG. (D) 0.01 mg/mL horse IgG.**

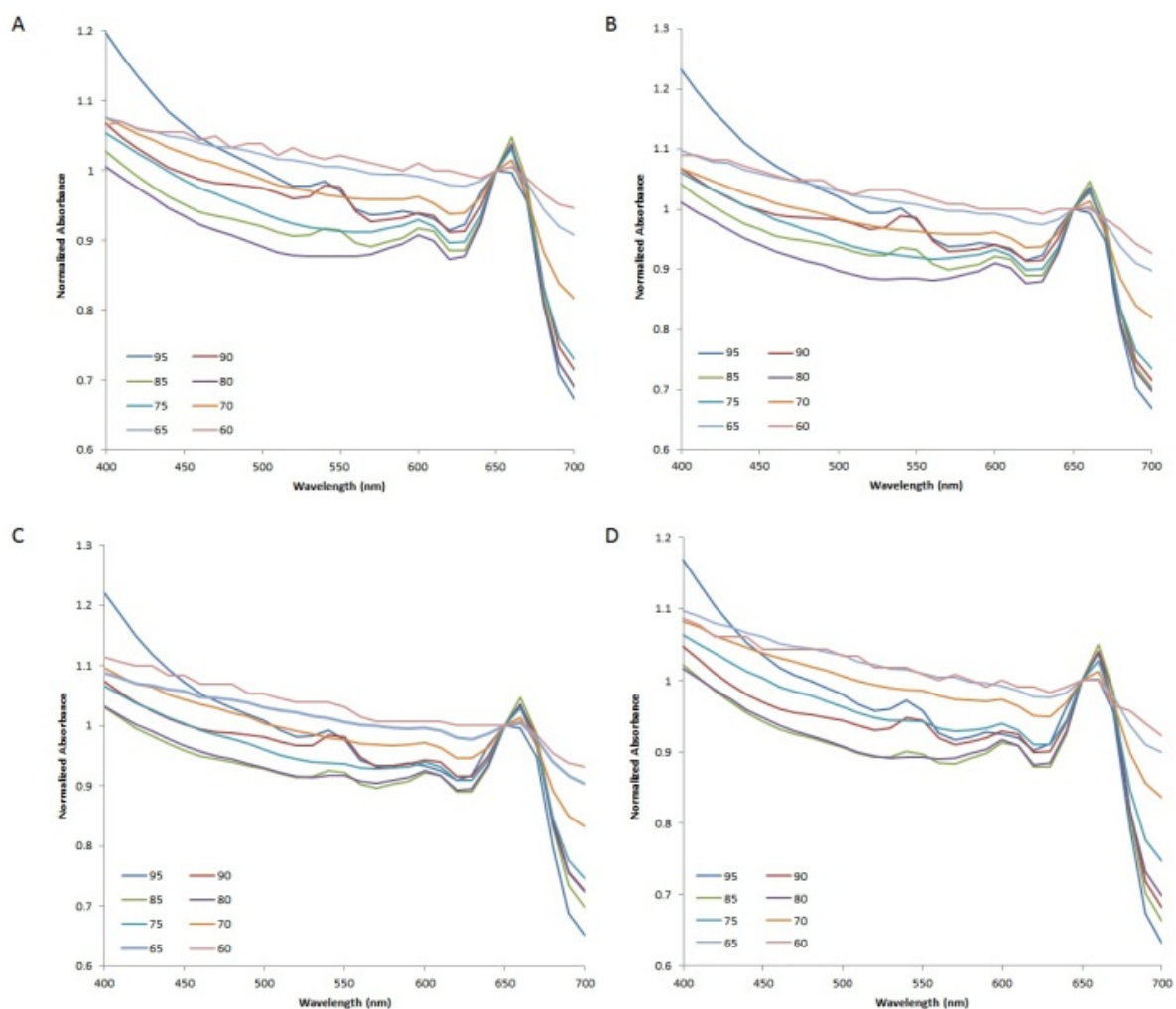


**Figure 7. Absorption spectra of Lys-PCDA/SPION sensors of varying PDA wt%, normalised to 650 nm. (A) 1 mg/mL horse IgG. (B) 0.5 mg/mL horse IgG. (C) 0.1 mg/mL horse IgG. (D) 0.01 mg/mL horse IgG.**

The absorption spectra are shown in Figure 7 and highlight the significance of PDA concentrations used in the sensor fabrication to achieving optimal performance. Spectra for 60-65 wt% appeared very similar to the controls in PBS (Figure 5(B)), indicating that not enough PDA was present to produce a colour response. At the lower PDA concentrations of 70-80 wt%, little colour change was visually observed and appearance of a peak at 540 nm, indicative of the red state, was not detected, signifying no sensing had likely occurred. This was expected after sensor fabrication, as the 60-80 wt% sensors did not appear as blue as previously described PDA-based sensors. In comparison, 85-95 wt% sensors all showed the appearance of peaks at 540 nm, supporting the visual observations.

Of interesting note is that the 90-95 wt% sensors showed the largest peaks at 540 nm among the colour response compositions despite the loss of some of the sensor particles during the wash steps.

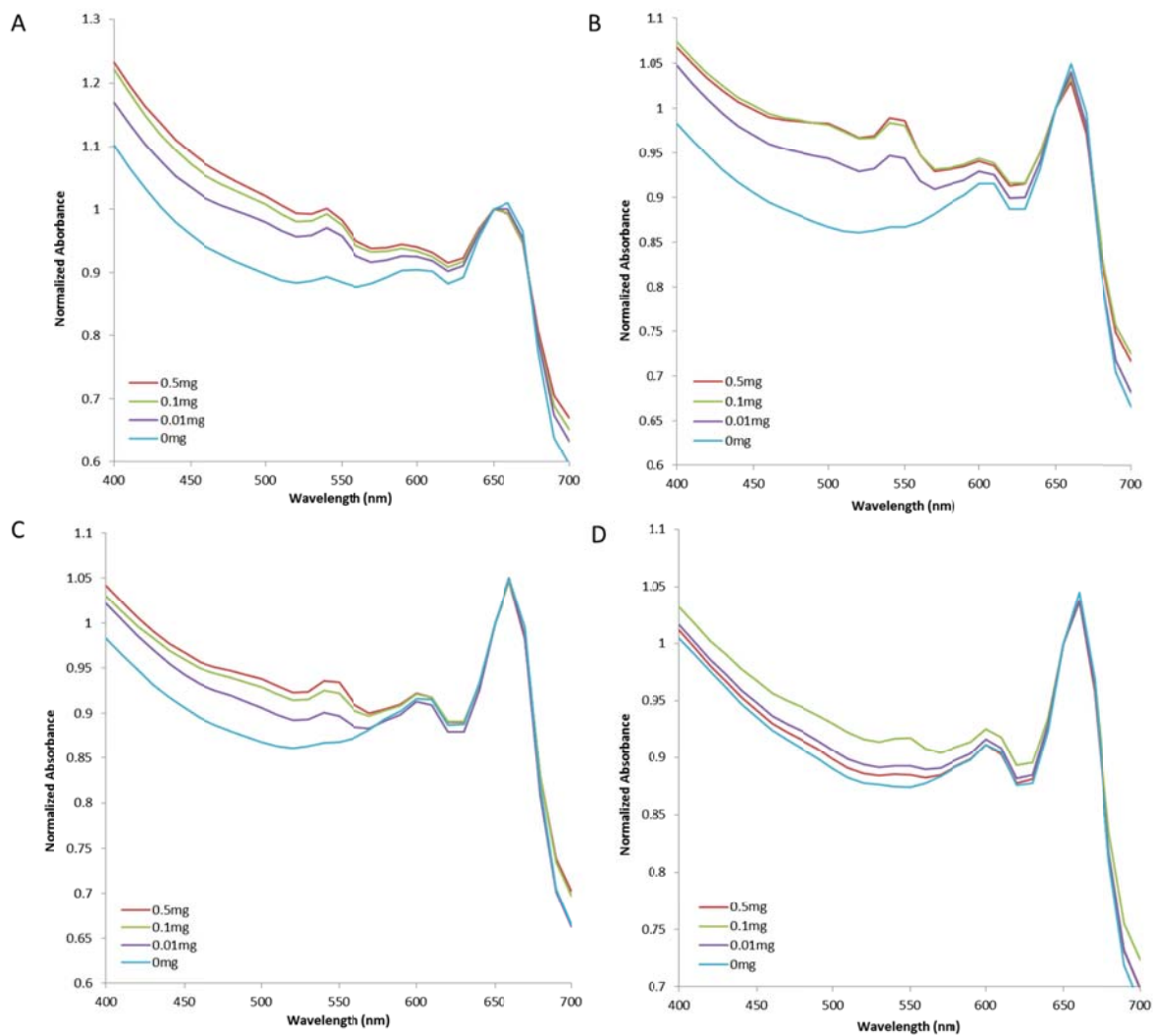


**Figure 8. Absorption spectra of Lys-PCDA/SPION sensors of 80-95 wt% PDA, normalised to 650 nm, in increasing horse IgG concentrations. (A) 95 wt% PDA. (B) 90 wt% PDA. (C) 85 wt% PDA. (D) 80 wt% PDA.**

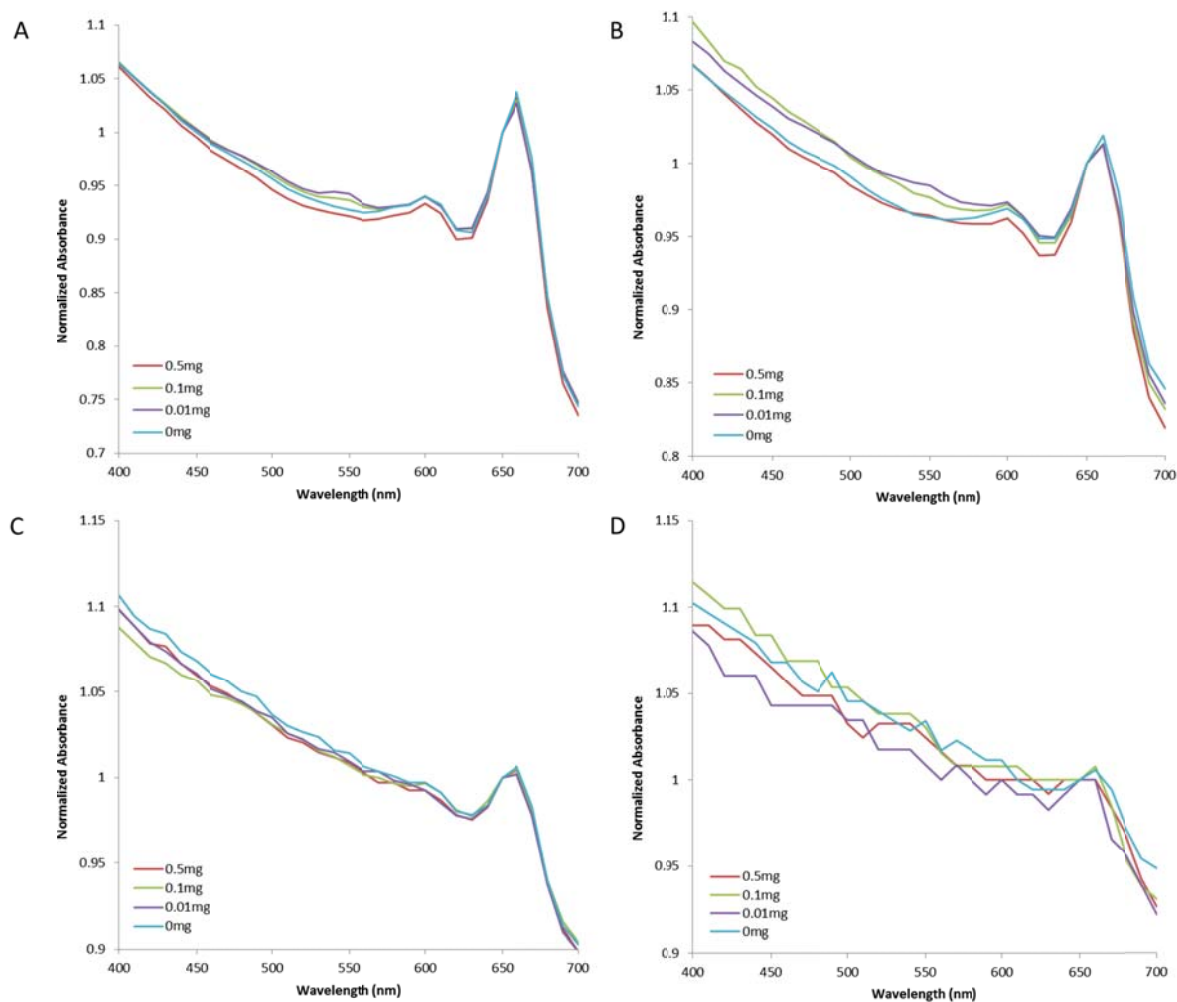


**Figure 9. Absorption spectra of Lys-PCDA/SPION sensors of 60-75 wt% PDA, normalised to 650 nm, in increasing horse IgG concentrations. (A) 75 wt% PDA. (B) 70 wt% PDA. (C) 65 wt% PDA. (D) 60 wt% PDA.**

Comparison of individual sensor compositions among the various horse IgG concentrations supports the previous observations on the optimal amount of PDA (Figures 8 and 9). Spectra of the 60-65 wt% sensors appeared mostly as noise, while the 70-80 wt% sensors showed no reliable trends. In contrast, the 85-95 wt% PDA sensors demonstrated a colorimetric response to increasing concentrations of horse IgG. Of significant note is the marked difference between 0 and 0.01 mg/mL and between 0.01 mg/mL and the larger concentrations. In this work, 0.01 mg/mL was specifically chosen to demonstrate the potential applicability of the Lys-PCDA/SPION sensor for biomarker-

based diagnosis of critical illnesses such as sepsis. Serum concentrations greater than 0.01 mg/mL of C-reactive protein (CRP), a commonly used biomarker for diagnosing sepsis<sup>37</sup> and several other illnesses,<sup>38</sup> are indicative of sepsis.<sup>41</sup> The 85-95 wt% sensors all demonstrated different colorimetric responses when incubated with 0.01 mg/mL, compared to the higher concentrations of target analyte. Quantitatively, the 85 wt% PDA sensor demonstrated a 2.01% and 1.70% colorimetric response at 0.5 and 0.1 mg/mL when normalised against the colorimetric response at 0.01 mg/mL, while the 90 and 95 wt% sensors showed respective colorimetric responses of 1.48% and 1.42%, and 1.37% and 1.27% (Figure 10).

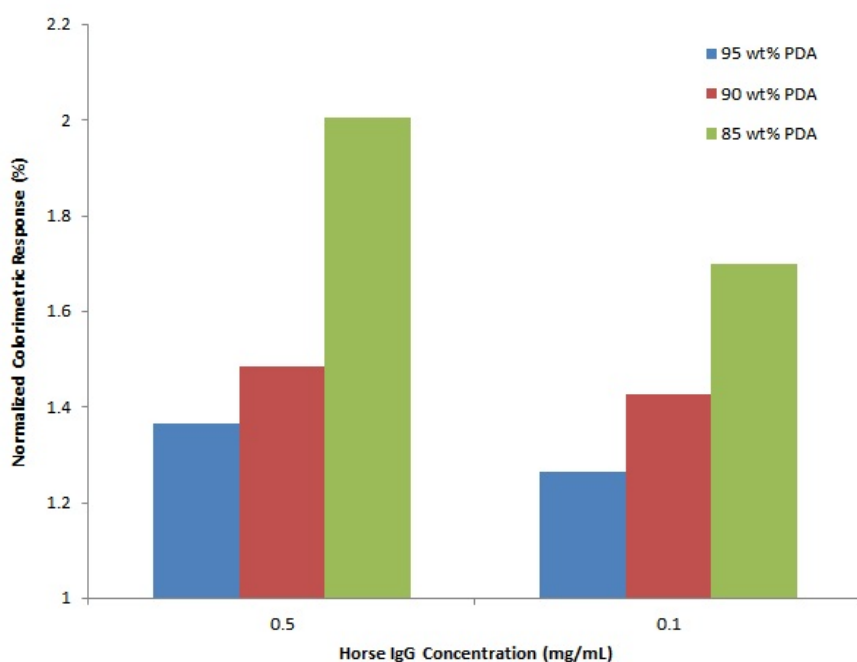


**Figure 10. Colorimetric response of 85, 90 and 95 wt% PDA compositions of Lys-PCDA/SPION sensors, normalised against the colorimetric response at 0.01 mg/mL horse IgG.**

Based on the results, the optimal ratio of Lys-PCDA to hydrophobic SPIONs to use during sensor fabrication is 85 wt% to achieve optimal sensor performance. At PDA ratios below 80 wt%, the sensors demonstrate weak colorimetric sensing properties, likely a result of insufficient amounts of PDA in the system. At lower ratios below 65 wt%, the insufficient amount of Lys-PCDA hinders both the colorimetric sensing and magnetic separability properties. While high ratios of 90-95 wt%

PDA demonstrate greater visual colour responsiveness, complete magnetic retention was not observed and the reduction in sensor particles resulted in lower than expected measurable colorimetric responses, especially when compared against the CR% values at 0.01 mg/mL.

## **5.4 Conclusions**

In summary, previously described Lys-PCDA/SPION biosensors for point-of-care testing applications was optimised, with the 85 wt% PDA composition showing the best performance. Additionally, the sensors successfully demonstrated a lower detection limit of 0.01 mg/mL, significantly better than the previously reported 0.5 mg/mL. Horse IgG/anti-horse IgG binding was used in this work as a cost-effective optimisation of the biosensor and to demonstrate the versatility of the biosensor for detecting different target analytes. The optimisation of the biosensor presented in this work highlights the sensor as a potential diagnostic platform to meet the urgent need of point-of-care testing sensors.

## 6.0 Conclusions and Recommendations

### 6.1 Concluding Summary

This thesis began with an overview of the requirements and benefits of point-of-care testing (POCT) systems for diagnosing critical illnesses, with a specific focus on sepsis. A comprehensive literature review followed on the most commonly studied biomarkers of sepsis, with a focus on their diagnostic relevancy and applicability to POCT systems, to establish the serum protein levels that require detection. Available systems were also identified to determine the diagnostic issues not addressed by current biomarker-based sensors. From this research, the following research objectives were established: 1) to develop a biosensor capable of colorimetric detection of small concentrations of biomolecules and capture of target analytes from complex solutions through simple magnetic separation, and 2) to demonstrate tuning of the colorimetric response and versatility of the sensor for detecting different analytes. From these objectives, polydiacetylenes, a class of conjugated polymers, were chosen for colorimetric sensing because of their unique optical property of transitioning from blue to red in response to receptor-ligand interactions. Superparamagnetic iron oxide was chosen to form the magnetically separable core of the sensor because of their simple synthesis and demonstrated superparamagnetism.

Using the concept of nanoprecipitation, polydiacetylene-coated SPION sensor particles were successfully developed and functionalised for biomolecule detection and capture from a complex antiserum solution. The benefits of magnetic separation in the sensor design were also demonstrated. A lower detection limit of 0.5 mg/mL was achieved, applicable to many sensing application, but required a more sensitive lower detection limit for sepsis biomarker detection.

Tuning of the biosensor's colorimetric response was achieved by varying the ratio of PDA to SPION during sensor fabrication, showing improved colour responsiveness with increasing PDA concentrations. Low PDA concentrations resulted in poor magnetic separability and colorimetric performance, while using very high PDA concentrations resulted in some loss of sensor retention during magnetic separation, resulting in an optimal ratio of 85 wt% amphiphilic PDA/15 wt% hydrophobic SPIONs being determined. In addition, the versatility of the biosensor was demonstrated by utilising a different receptor-ligand system, and the lower detection limit was improved to 0.01 mg/mL, a diagnostically relevant concentration when using C-reactive protein to diagnose sepsis.

This work has been significant because it establishes a new sensing platform with the capacity to serve in a wide range of POCT applications, demonstrating simple operation and fabrication and visually observable colorimetric detection. The demonstrated target versatility of the biosensor is indicative of its potential adaption to other sensing applications beyond disease diagnosis, ranging from personal care to food safety.

## **6.2 Recommendations for Future Work**

With the demonstration of Lys-PCDA/SPION sensor particles as a viable platform for point-of-care testing, further experimentation could be pursued to achieve specific colour responses to specific biomarker concentration ranges. Additionally, achieving even lower detection limits to allow the sensing of biomarkers in ng/mL concentrations would be a major milestone in the development of POCT systems for sepsis, given the large demand for diagnostic systems with increasing sensitivity. This could be achieved by determining the optimal amount of receptors to functional a given sensor surface area. Exploring the effects of incorporating different materials into the amphiphilic PDA surface, as well as using other polar molecules to modify the native polydiacetylene, may lead to enhanced colorimetric properties. For example, previous studies on PDA-based sensors have included phospholipids into PDA structures to adjust the amount of crosslinking between diacetylene monomers, while other studies have modified native PDA with glycolipids for detection of certain bacteria. The work in this thesis utilised readily available receptor and ligand materials to achieve cost-effective demonstrations of the biosensor's properties. The successful research presented here warrants that future experimentations should use receptors against specific biomarkers of sepsis, as well as receptors for biomarkers of other diseases and toxic environmental materials.

In summary, the significant works discussed in this thesis can be further developed by:

1. Exploring the inclusion of different materials within the PDA surface of Lys-PCDA/SPION sensors.
2. Investigating the effects of modifying native PDA with different polar molecules other than the lysine derivative currently used.
3. Establishing the optimal ratio of receptor molecules for a defined surface area of the biosensor.
4. Discovering new analytes that can be colorimetrically detected with the biosensor by incorporating different receptor molecules.

## Appendix A

### Synthesis of Oleic Acid-Coated Superparamagnetic Iron Oxide Particles

Oleic acid-coated superparamagnetic iron oxide particles (OA-SPIONs) were synthesised using a co-precipitation method (Scheme A1). 13 g of iron(II) chloride and 9 g of iron(III) sulfate were dissolved together in 25 mL distilled water under nitrogen using continuous magnetic stirring. Once dissolved, the solution was heated to 70°C, during which 25 mL of ammonium hydroxide was added, followed immediately by 3 g of oleic acid (technical grade, 90%). Once the solution reached 70°C, the solution was heated for 1 hour, then heated at 85°C until black aggregates formed. The OA-SPIONs were extracted with HPLC-grade chloroform, then washed more than 6 times with HPLC-grade ethanol via magnetic separation to remove excess oleic acid. The final product was dried under streaming nitrogen. Hydrophobicity was confirmed by dispersion in a chloroform and water solution (Figure A1). TEM analysis of the OA-SPIONs revealed individual particle sizes ranging from 5-14 nm.

#### Scheme A1

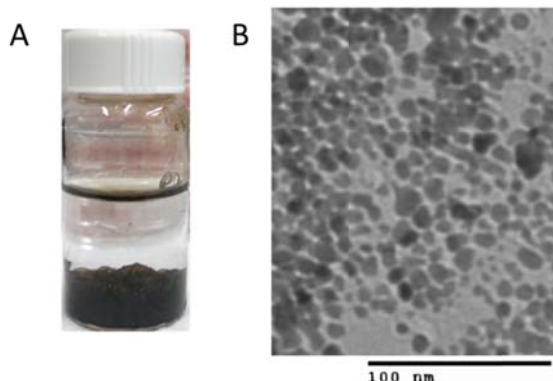
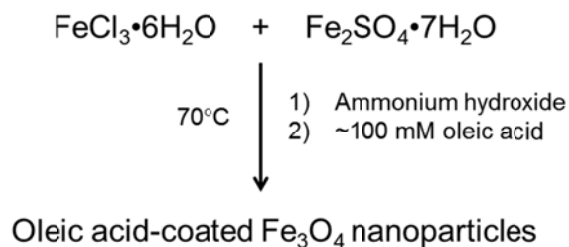


**Figure A1. Analysis of OA-SPIONs** (A) Dispersion in water/chloroform mixture. (B) Size analysis by TEM.

### Synthesis of Lys-PCDA

The diacetylene monomer 10,12-pentacosadiynoic acid (PCDA) (Alfa Aesar) was modified with a hydrophilic lysine derivative,  $N_{\alpha},N_{\alpha}$ -bis(carboxymethyl)-L-lysine hydrate (BCML) (Sigma Aldrich) via a two-step coupling chemistry with 1-ethyl-3-(3-dimethylaminopropyl) carbodiimide (EDC) and N-hydroxysuccinimide (NHS) (Figure A2(A)). PCDA was dissolved in a 1:1 mixture of chloroform (HPLC-grade) and ethanol with at least 1.25 molar excess of NHS and 1.5 molar excess of EDC and stirred overnight to form an amine-reactive PCDA intermediate. The intermediate was washed with 20% w/v brine and extracted with chloroform, dried over anhydrous sodium sulfate to form a white powder, then dissolved in tetrahydrofuran (THF) to form a 20 mM solution. A 1.2 molar excess of BCML was added to Milli-Q water to 20 mg/mL and dissolved under stirring via dropwise addition of triethylamine (TEA). The entire BCML solution was added dropwise to the NHS-activated PCDA in THF under stirring over a duration of 30 minutes with a syringe pump, then stirred sealed overnight. 1 M hydrochloric acid (HCl) was added dropwise to the solution until a white emulsion formed ( $\sim$ pH 1), concentrated with a rotary evaporator, washed with 1 M HCl several times, and dried. Finally, the recovered precipitate was dissolved in a 1:1 mixture of chloroform and methanol, filtered with 0.45  $\mu$ m PTFE membrane, and dried to produce a purplish white powder. Appearance of peaks at 1.98, 2.67, 2.77, 3.36, and 7.68 ppm and the increased intensity at 2.50 ppm on the Lys-PCDA spectrum indicated the presence of successful conjugation of BCML (Figure A2(B)).

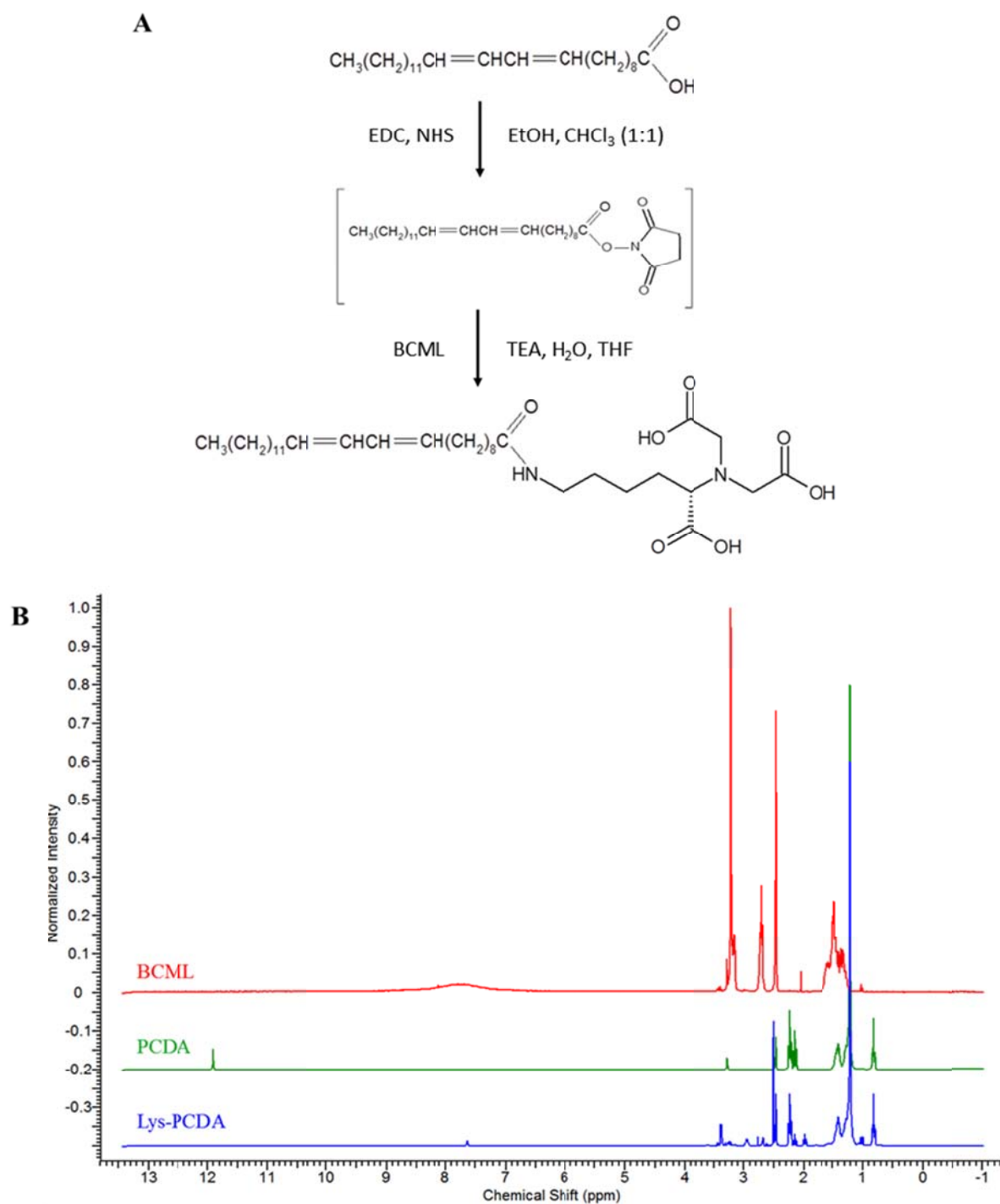


**Figure A2. Synthesis of lysine-modified 10,12-pentacosadiynoic acid.** (A) The synthesis involves a two-step EDC/NHS conjugation process. (B)  $^1\text{H}$  NMR spectra of BCML, PCDA, and Lys-PCDA.

### Assay of rabbit anti-BSA antiserum

Rabbit anti-BSA antiserum (Rockland Immunochemicals Inc.) was reconstituted according to manufacturer's instructions, then washed twice with 0.1M PBS buffer, pH 7.2 (Thermo Scientific) using Amicon Ultra-15 10 kDA MWCO tubes (EMD Millipore), centrifuged at 4000 xg for 20 minutes, to remove sodium azide. The antiserum solution was diluted with PBS buffer to the concentrations of 80, 40, 20, 10, 5, 2, and 1 mg/mL total antiserum protein. Manufacturer specifications indicated ~10% of the total antiserum protein was anti-BSA antibodies.

The BSA-functionalised Lys-PCDA/SPION particles were mixed with 1 mL aliquots of each anti-BSA antiserum concentration, as well as negative controls of PBS buffer and of 20 mg/mL purified lysozyme from chicken egg white (Sigma Aldrich) in PBS, in 7 mL scintillation vials. Mixing was monitored for the first hour, then left to run overnight. Total mixing time was 18.5 hours. The positive control showed no visible change. Each anti-BSA sample of particles was washed with PBS buffer 4 times, until the presence of foaming was no longer observed, then dispersed in 0.9 mL PBS buffer. 3 0.3 mL aliquots were taken from each sample and added to a sterile 96-well polypropylene microwell plate (Grenier Bio-One). Visible absorbance spectra were recorded (400-700 nm) in 10 nm increments with a Biotek Epoch UV-visible spectrophotometer. Absorbance readings were performed 3 times, for a total of 3 triplicates per sample.

To calculate the colorimetric response (CR%), the absorbance values at 550 and 650 nm were used in the following equations:

$$CR \% = \frac{(PB_0 - PB_1)}{PB_0} \times 100\%$$

where  $PB = A_{blue}/(A_{blue} + A_{red})$ ,  $A$  was the UV-visible absorbance value of the particle's "blue" state at 650 nm or the "red" state at 550 nm, and  $PB_0$  and  $PB_1$  were the respective colorimetric ratios of the particles before and after the assay. The calculated values are displayed in Table A1.

**Table A1. Calculation of colorimetric values (CR %).**

Anti-BSA (mg/mL)	8	4	2	1	0.5	0
A <sub>550</sub>	0.544556	0.629222	0.458778	0.560778	0.549778	0.593667
A <sub>650</sub>	0.540444	0.626444	0.457667	0.561111	0.553111	0.599222
PB <sub>1</sub>	0.498105	0.498894	0.499394	0.500149	0.501511	0.502329
PB <sub>0</sub>	0.502329	0.502329	0.502329	0.502329	0.502329	0.502329
CR %	0.840712	0.683758	0.584243	0.43399	0.162728	0

OriginPro 8.5 was used to perform regression analysis, using the non-linear curve fit tool. A hyperbolic curve achieved the best fit of the data (Figure A3).

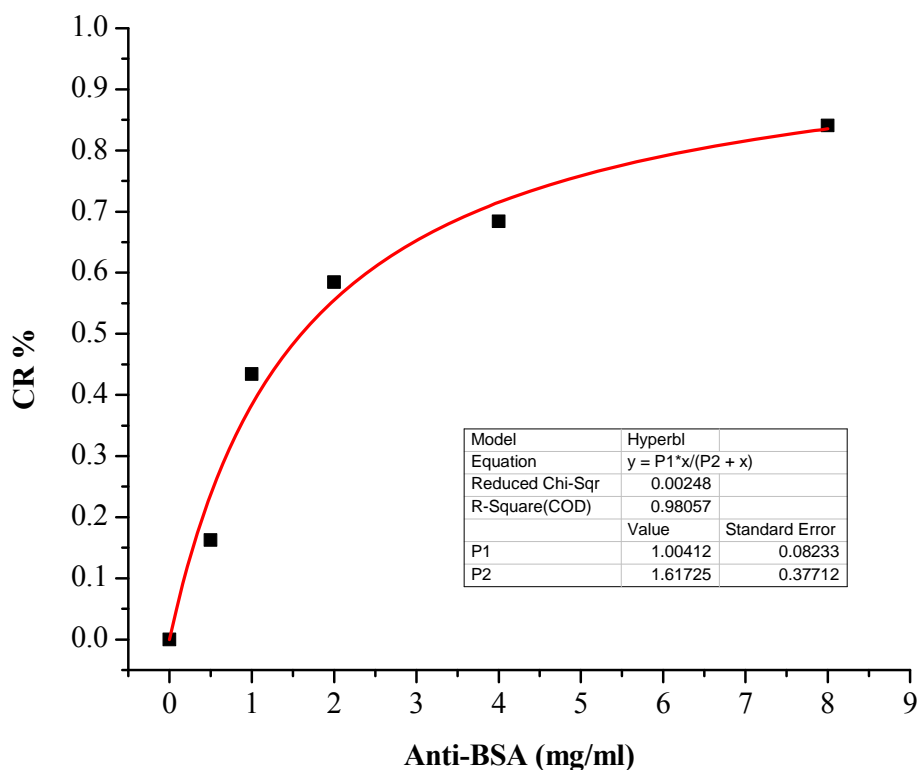


**Figure A3. Regression analysis of colorimetric response values.**

## Permissions

Expert Reviews Ltd., grant permission to reuse the manuscript “Early diagnosis of sepsis using serum biomarkers” published in Expert Review of Molecular Diagnostics, June 2011, Vol. 11, No. 5, Pages 487-496 within the publication of this thesis, in print and electronic media.

Notes and conditions:

1. This permission is granted free of charge, for one-time use only.
2. Expert Reviews Ltd grant the publisher non-exclusive world rights to publish the content in the publication specified above.
3. Expert Reviews Ltd retains copyright ownership of the content.
4. Permission is granted on a one-time basis only. Separate permission is required for any further use or edition.
5. The publisher will make due acknowledgement of the original publication wherever they republish the content: citing the author, content title, publication name and Expert Reviews Ltd as the original publisher.
6. The publisher will not amend, abridge, or otherwise change the content without authorization from Expert Reviews Ltd.
7. Permission does not include any copyrighted material from other sources that may be incorporated within the content.
8. Failure to comply with the conditions above will result in immediate revocation of the permission here granted.

## Bibliography

1. M. Doherty, R. S. Wallis, A. Zumla and W. H. O. T. D. Res, *Current opinion in pulmonary medicine*, 2009, **15**, 181-187.
2. P. Yager, G. J. Domingo and J. Gerdes, *Annual Review of Biomedical Engineering*, 2008, **10**, 107-144.
3. E. Aguilera-Herrador, M. Cruz-Vera and M. Valcarcel, *Analyst*, 2010, **135**, 2220-2232.
4. R. W. Peeling and D. Mabey, *Clinical Microbiology and Infection*, 2010, **16**, 1062-1069.
5. S. Mtapuri-Zinyowera, M. Chideme, D. Mangwanya, O. Mugurungi, S. Gudukeya, K. Hatzold, A. Mangwiro, G. Bhattacharya, J. Lehe and T. Peter, *J aids-Journal of Acquired Immune Deficiency Syndromes*, 2010, **55**, 1-7.
6. P. Wang, Z.-T. Yang, Y.-G. He and C.-M. Shu, *Reviews in Medical Microbiology*, 2010, **21**, 39-43.
7. I. A. M. Kauss, C. M. C. Grion, L. T. Q. Cardoso, E. H. T. Anami, L. B. Nunes, G. L. Ferreira, T. Matsuo and A. M. Bonametti, *Brazilian Journal of Infectious Diseases*, 2010, **14**, 264-270.
8. P. Hunter, *EMBO reports*, 2006, **7**, 667-669.
9. D. C. Angus, W. T. Linde-Zwirble, J. Lidicker, G. Clermont, J. Carcillo and M. R. Pinsky, *Critical care medicine*, 2001, **29**, 1303-1310.
10. M. Cetinkaya, H. Ozkan, N. Koksall, S. Celebi and M. Hacimustafaoglu, *Journal of Perinatology*, 2009, **29**, 225-231.
11. E. Zecca, G. Barone, M. Corsello, C. Romagnoli, E. Tiberi, C. Tirone and G. Vento, *Clinical Chemistry and Laboratory Medicine*, 2009, **47**, 1081-1084.
12. I. O. Ipek, M. Saracoglu and A. Bozaykut, *Journal of Maternal-Fetal & Neonatal Medicine*, 2010, **23**, 617-621.
13. M. A. C. Rego, F. E. Martinez, J. Elias and M. M. Mussi-Pinhata, *Journal of perinatal medicine*, 2010, **38**, 527-533.
14. R. S. Watson, J. A. Carcillo, W. T. Linde-Zwirble, G. Clermont, J. Lidicker and D. C. Angus, *American Journal of Respiratory and Critical Care Medicine*, 2003, **167**, 695-701.
15. P. Cardelli, M. Ferraironi, R. Amode, F. Tabacco, R. A. De Blasi, M. Nicoletti, R. Sessa, A. Petrucca, A. Costante and P. Cipriani, *International Journal of Immunopathology and Pharmacology*, 2008, **21**, 43-49.

16. B. L. Cheng, G. H. Xie, S. L. Yao, X. M. Wu, Q. L. Guo, M. N. Gu, Q. Fang, Q. P. Xu, D. X. Wang, Y. H. Jin, S. Y. Yuan, J. L. Wang, Z. H. Du, Y. B. Sun and X. M. Fang, *Critical care medicine*, 2007, **35**, 2538-2546.
17. M. J. Sankar, R. Agarwal, A. K. Deorari and V. K. Paul, *Indian journal of pediatrics*, 2008, **75**, 261-266.
18. S. S. Desmet, *Intensive care medicine*, 1994, **20**, 300-304.
19. S. Arnon and I. Litmanovitz, *Current opinion in infectious diseases*, 2008, **21**, 223-227.
20. A. A. H. Zeitoun, S. S. Gad, F. M. Attia, A. S. Abu Maziad and E. F. Bell, *Scandinavian journal of infectious diseases*, 2010, **42**, 299-305.
21. K. L. Becker, R. Snider and E. S. Nylen, *Critical care medicine*, 2008, **36**, 941-952.
22. J. S. Oh, S. U. Kim, Y. M. Oh, S. M. Choe, G. H. Choe, S. P. Choe, Y. M. Kim, T. Y. Hong and K. N. Park, *American Journal of Emergency Medicine*, 2009, **27**, 859-863.
23. A. Lannergard, A. Larsson, G. Friman and U. Ewald, *Acta Paediatrica*, 2008, **97**, 1061-1065.
24. D. Maubon, R. Hamidfar-Roy, S. Courby, A. Vesin, M. Maurin, P. Pavese, N. Ravel, C. E. Bulabois, J. P. Brion, H. Pelloux and J. F. Timsit, *Journal of Infection*, 2010, **61**, 335-342.
25. A. Martini, L. Gottin, N. Menestrina, V. Schweiger, D. Simion and J. L. Vincent, *Journal of Infection*, 2010, **60**, 425-430.
26. M. von Lilienfeld-Toal, L. E. Lehmann, A. D. Raadts, C. Hahn-Ast, K. S. Orlopp, G. Marklein, I. Purr, G. Cook, A. Hoeft, A. Glasmacher and F. Stuber, *Journal of clinical microbiology*, 2009, **47**, 2405-2410.
27. C. Pierrakos and J. L. Vincent, *Critical Care*, 2010, **14**.
28. J. Bille, *Current opinion in critical care*, 2010, **16**, 460-464.
29. J. C. Marshall, K. Reinhart and F. Int Sepsis, *Critical care medicine*, 2009, **37**, 2290-2298.
30. S. Arnon, I. Litmanovitz, R. H. Regev, S. Bauer, R. Shainkin-Kestenbaum and T. Dolfon, *Journal of Perinatology*, 2007, **27**, 297-302.
31. H. Ugarte, E. Silva, D. Mercan, A. De Mendonca and J. L. Vincent, *Critical care medicine*, 1999, **27**, 498-504.
32. K. E. Kim and J. Y. Han, *Korean Journal of Laboratory Medicine*, 2010, **30**, 153-159.
33. D. E. Chiriboga, Y. S. Ma, W. J. Li, E. J. Stanek, J. R. Hebert, P. A. Merriam, E. S. Rawson and I. S. Ockene, *Clinical chemistry*, 2009, **55**, 313-321.
34. L. Simon, F. Gauvin, D. K. Amre, P. Saint-Louis and J. Lacroix, *Clinical Infectious Diseases*, 2004, **39**, 206-217.

35. M. Groselj-Grenc, A. Ihan, M. Pavcnik-Arnol, A. N. Kopitar, T. Gmeiner-Stopar and M. Derganc, *Intensive care medicine*, 2009, **35**, 1950-1958.
36. A. Galetto-Lacour, S. A. Zamora and A. Gervaix, *Pediatrics*, 2003, **112**, 1054-1060.
37. A. G. Lacour, A. Gervaix, S. A. Zamora, L. Vadas, P. R. Lombard, J. M. Dayer and S. Suter, *European journal of pediatrics*, 2001, **160**, 95-100.
38. D. I. Agapakis, D. Tsantilas, P. Psarris, E. V. Massa, P. Kotsaftis, K. Tziomalos and A. I. Hatzitolios, *Respirology*, 2010, **15**, 796-803.
39. A. Enguix, C. Rey, A. Concha, A. Medina, D. Coto and M. A. Dieguez, *Intensive care medicine*, 2001, **27**, 211-215.
40. J. D. M. Edgar, V. Gabriel, J. R. Gallimore, S. A. McMillan and J. Grant, *Bmc Pediatrics*, 2010, **10**.
41. A. Lannergard, G. Friman, U. Ewald, L. Lind and A. Larsson, *Acta Paediatrica*, 2005, **94**, 1198-1202.
42. J. R. Fioretto, J. G. Martin, C. S. Kurokawa, M. F. Carpi, R. C. Bonatto, M. A. de Moraes and S. M. Q. Ricchetti, *Inflammation Research*, 2010, **59**, 581-586.
43. B. L. dos Anjos and H. Z. W. Grotto, *Clinical Chemistry and Laboratory Medicine*, 2010, **48**, 493-499.
44. C. S. M. O. Nijhuis, E. Vellenga, S. M. G. J. Daenen, W. T. A. van der Graaf, J. A. Gietema, H. J. M. Groen, W. A. Kamps and E. S. J. M. de Bont, *Intensive care medicine*, 2003, **29**, 2157-2161.
45. G. L. Petrikos, S. A. Christofilopoulou, N. K. Tentolouris, E. A. Charvalos, C. J. Kosmidis and G. L. Daikos, *European Journal of Clinical Microbiology & Infectious Diseases*, 2005, **24**, 272-275.
46. S. Gibot, M. N. Kolopp-Sarda, M. C. Bene, A. Cravoisy, B. Levy, G. C. Faure and P. E. Bollaert, *Annals of Internal Medicine*, 2004, **141**, 9-15.
47. T. Kajiya, K. Orihara, S. Hamasaki, R. Oba, H. Hirai, K. Nagata, T. Kumagai, S. Ishida, N. Oketani, H. Ichiki, S. Kuwahata, S. Fujita, N. Uemura and C. Tei, *Journal of Infection*, 2008, **57**, 249-259.
48. A. Lannergard, A. Viberg, O. Cars, M. O. Karlsson, M. Sandstrom and A. Larsson, *Scandinavian journal of infectious diseases*, 2009, **41**, 663-671.

49. Y. E. Claessens, J. Schmidt, E. Batard, S. Grabar, D. Jegou, P. Hausfater, G. Kierzek, S. Guerin, J. L. Pourriat, J. F. Dhainaut, C. Ginsburg and B. I. S. S. Grp, *Clinical Microbiology and Infection*, 2010, **16**, 753-760.
50. Y. E. Claessens, T. Mathevon, G. Kierzek, S. Grabar, D. Jegou, E. Batard, C. Loyer, A. Davido, P. Hausfater, H. Robert, L. Lavagna-Perez, B. Bernot, P. Plaisance, C. Leroy and B. Renaud, *Intensive care medicine*, 2010, **36**, 799-809.
51. J. T. Whicher, R. E. Chambers, J. Higginson, L. Nashef and P. G. Higgins, *Journal of clinical pathology*, 1985, **38**, 312-316.
52. J. K. Quint, G. C. Donaldson, J. J. P. Goldring, R. Baghai-Ravary, J. R. Hurst and J. A. Wedzicha, *Chest*, 2010, **137**, 812-822.
53. A. Nakamura, H. Wada, M. Ikejiri, T. Hatada, H. Sakurai, Y. Matsushima, J. Nishioka, K. Maruyama, S. Isaji, T. Takeda and T. Nobori, *Shock*, 2009, **31**, 586-591.
54. J. N. Deis, C. B. Creech, C. M. Estrada and T. J. Abramo, *Pediatric emergency care*, 2010, **26**, 51-63.
55. H. M. Dong, W. Shu, T. C. Liu, S. H. Wang, G. F. Lin, M. Li and Y. S. Wu, *Hybridoma*, 2010, **29**, 189-194.
56. P. Schuetz, M. Christ-Crain, A. R. Huber and B. Muller, *Clinical biochemistry*, 2010, **43**, 341-344.
57. S. Manzano, B. Bailey, J. B. Girodias, J. Cousineau, E. Delvin and A. Gervaix, *Clinical biochemistry*, 2009, **42**, 1557-1560.
58. M. Limper, M. D. de Kruif, A. J. Duits, D. P. M. Brandjes and E. C. M. van Gorp, *Journal of Infection*, 2010, **60**, 409-416.
59. H. Oshita, J. Sakurai and M. Kamitsuna, *Journal of Microbiology Immunology and Infection*, 2010, **43**, 222-227.
60. R. G. Wunderink, *Clinical Infectious Diseases*, 2010, **51**, S126-S130.
61. F. Dubos, F. Moulin, V. Gajdos, N. De Suremain, S. Biscardi, P. Lebon, J. Raymond, G. Breart, D. Gendrel and M. Chalumeau, *Journal of Pediatrics*, 2006, **149**, 72-76.
62. Y. Sakr, C. Sponhoz, F. Tuche, F. Brunkhorst and K. Reinhart, *Infection*, 2008, **36**, 396-407.
63. M. Pavic, A. Bronic and L. M. Kopicinovic, *Biochemia Medica*, 2010, **20**, 236-241.
64. D. N. Gilbert, *Journal of clinical microbiology*, 2010, **48**, 2325-2329.
65. M. J. Schultz and R. M. Determann, *Medical Science Monitor*, 2008, **14**, RA241-RA247.

66. C. P. Schneider, Y. Yilmaz, A. Kleespies, K. W. Jauch and W. H. Hartl, *Shock*, 2009, **31**, 568-573.
67. A. F. Lopez, C. L. Cubells, J. J. G. Garcia, J. F. Pou and E. Spanish Soc Pediat, *Pediatric Infectious Disease Journal*, 2003, **22**, 895-903.
68. D. Kelly, S. Q. Khan, O. Dhillon, P. Quinn, J. Struck, I. B. Squire, J. E. Davies and L. L. Ng, *Biomarkers*, 2010, **15**, 325-331.
69. M. Christ-Crain and S. M. Opal, *Critical Care*, 2010, **14**.
70. J. P. Mira, A. Max and P. R. Burgel, *Critical Care*, 2008, **12**.
71. M. Cetinkaya, H. Ozkan, N. Koksall, O. Akaci and T. Ozgur, *Pediatric surgery international*, 2010, **26**, 835-841.
72. M. C. Arendrup, O. J. Bergmann, L. Larsson, H. V. Nielsen, J. O. Jarlov and B. Christensson, *Clinical Microbiology and Infection*, 2010, **16**, 855-862.
73. M. Ellis, B. Al-Ramadi, R. Bernsen, J. Kristensen, H. Alizadeh and U. Hedstrom, *Journal of medical microbiology*, 2009, **58**, 606-615.
74. B. Sendid, T. Jouault, R. Coudriau, D. Camus, F. Odds, M. Tabouret and D. Poulain, *Journal of clinical microbiology*, 2004, **42**, 164-171.
75. P. C. Ng, K. Li, K. M. Chui, T. F. Leung, R. P. O. Wong, W. C. W. Chu, E. Wong and T. F. Fok, *Pediatric research*, 2007, **61**, 93-98.
76. K. C. Sumino, M. J. Walter, C. L. Mikols, S. A. Thompson, M. Gaudreault-Keener, M. Q. Arens, E. Agapov, D. Hormozdi, A. M. Gaynor, M. J. Holtzman and G. A. Storch, *Thorax*, 2010, **65**, 639-644.
77. J. A. Wang, P. P. Wang, G. J. Xiang and X. B. Hu, *Hepatobiliary & Pancreatic Diseases International*, 2010, **9**, 280-286.
78. M. Lagging, A. I. Romero, J. Westin, G. Norkrans, A. P. Dhillon, J. M. Pawlotsky, S. Zeuzem, M. von Wagner, F. Negro, S. W. Schalm, B. L. Haagmans, C. Ferrari, G. Missale, A. U. Neumann, E. Verheij-Hart, K. Hellstrand and D.-H. S. Grp, *Hepatology*, 2006, **44**, 1617-1625.
79. M. Pavcnik-Arnol, S. Hojker and M. Derganc, *Intensive care medicine*, 2007, **33**, 1025-1032.
80. J. Nuutila, U. Hohenthal, L. Laitinen, P. Kotilainen, A. Rajamaki, J. Nikoskelainen and E. M. Lilius, *Journal of immunological methods*, 2007, **328**, 189-200.
81. J. Nuutila, *Current opinion in infectious diseases*, 2010, **23**, 268-274.

82. J. Cid, R. Aguinaco, R. Sanchez, G. Garcia-Pardo and A. Llorente, *Journal of Infection*, 2010, **60**, 313-319.
83. J. J. M. L. Hoffmann, *Clinical Chemistry and Laboratory Medicine*, 2009, **47**, 903-916.
84. P. Chourrout, *Medecine Nucleaire-Imagerie Fonctionnelle Et Metabolique*, 2008, **32**, 132-137.
85. J. Wilkins, J. R. Gallimore, G. A. Tennent, P. N. Hawkins, P. C. Limburg, M. H. Vanrijswijk, E. G. Moore and M. B. Pepys, *Clinical chemistry*, 1994, **40**, 1284-1290.
86. P. M. Bossuyt, J. B. Reitsma, D. E. Bruns, C. A. Gatsonis, P. P. Glasziou, L. M. Irwig, D. Moher, D. Rennie, H. C. W. de Vet and J. G. Lijmer, *Clinical chemistry*, 2003, **49**, 7-18.
87. P. M. Bossuyt, J. B. Reitsma, D. E. Bruns, C. A. Gatsonis, P. P. Glasziou, L. M. Irwig, J. G. Lijmer, D. Moher, D. Rennie, H. C. W. de Vet and S. Grp, *Clinical Chemistry and Laboratory Medicine*, 2003, **41**, 68-73.
88. H. J. Schunemann, A. D. Oxman, J. Brozek, P. Glasziou, P. Bossuyt, S. Chang, P. Muti, R. Jaeschke and G. H. Guyatt, *Evid Based Med*, 2008, **13**, 162-163.
89. H. J. Schunemann, A. H. J. Schunemann, A. D. Oxman, J. Brozek, P. Glasziou, R. Jaeschke, G. E. Vist, J. W. Williams, R. Kunz, J. Craig, V. M. Montori, P. Bossuyt and G. H. Guyatt, *Bmj*, 2008, **336**, 1106-1110.
90. J. F. Rusling, C. V. Kumar, J. S. Gutkind and V. Patel, *Analyst*, 2010, **135**, 2496-2511.
91. K. Lee, L. K. Povlich and J. Kim, *Analyst*, 2010, **135**, 2179-2189.
92. D. J. Ahn and J.-M. Kim, *Accounts of Chemical Research*, 2008, **41**, 805-816.
93. S. Abe, M. Schreiber, W. P. Su and J. Yu, *Physical Review B*, 1992, **45**, 9432-9435.
94. J. Liu, J. W. Y. Lam and B. Z. Tang, *Chemical Reviews*, 2009, **109**, 5799-5867.
95. S. Okada, S. Peng, W. Spevak and D. Charych, *Accounts of Chemical Research*, 1998, **31**, 229-239.
96. W. Thongmalai, T. Eaidkong, S. Ampornpun, R. Mungkarndee, G. Tumcharern, M. Sukwattanasinitt and S. Wacharasindhu, *Journal of Materials Chemistry*, 2011, **21**, 16391.
97. M. Schott, *The Journal of Physical Chemistry B*, 2006, **110**, 15864-15868.
98. S. Kolusheva, E. Wachtel and R. Jelinek, *Journal of Lipid Research*, 2003, **44**, 65-71.
99. Y. Scindia, L. Silbert, R. Volinsky, S. Kolusheva and R. Jelinek, *Langmuir*, 2007, **23**, 4682-4687.
100. O. Yarimaga, B. Yoon, D. Y. Ham, J. Lee, M. Hara, Y. K. Choi and J. M. Kim, *Journal of Materials Chemistry*, 2011, **21**, 18605-18612.

101. Y. Demikhovskiy, S. Kolusheva, M. Geyzer and R. Jelinek, *Journal of Colloid and Interface Science*, 2011, **364**, 428-434.
102. D. H. Charych, J. O. Nagy, W. Spevak and M. D. Bednarski, *Science*, 1993, **261**, 585-588.
103. P. Boullanger, D. Lafont, M. N. Bouchu, L. Jiang, T. Liu, W. Lu, C. X. Guo and J. Li, *Comptes Rendus Chimie*, 2008, **11**, 43-60.
104. E. C. M. Cabral, P. T. Hennies, C. R. D. Correia, R. L. Zollner and M. H. A. Santana, *Journal of Liposome Research*, 2003, **13**, 199-211.
105. A.-H. Lu, E. L. Salabas and F. Schüth, *Angewandte Chemie International Edition*, 2007, **46**, 1222-1244.
106. T. Neuberger, B. Schöpf, H. Hofmann, M. Hofmann and B. von Rechenberg, *Journal of Magnetism and Magnetic Materials*, 2005, **293**, 483-496.
107. K. Woo, J. Hong, S. Choi, H.-W. Lee, J.-P. Ahn, C. S. Kim and S. W. Lee, *Chemistry of Materials*, 2004, **16**, 2814-2818.
108. S. Kolusheva, R. Zadnard, T. Schrader and R. Jelinek, *Journal of the American Chemical Society*, 2006, **128**, 13592-13598.
109. A. C. dos Santos Pires, N. d. F. Ferreira Soares, L. H. Mendes da Silva, M. d. C. Hespanhol da Silva, M. V. De Almeida, M. Le Hyaric, N. J. de Andrade, R. F. Soares, A. B. Mageste and S. G. Reis, *Sensors and Actuators B-Chemical*, 2011, **153**, 17-23.
110. L. Cui, H. Xu, P. He, K. Sumitomo, Y. Yamaguchi and H. Gu, *Journal of Polymer Science Part A: Polymer Chemistry*, 2007, **45**, 5285-5295.
111. S. Kolusheva, R. Kafri, M. Katz and R. Jelinek, *Journal of the American Chemical Society*, 2001, **123**, 417-422.
112. N. Charoenthai, T. Pattanatornchai, S. Wacharasindhu, M. Sukwattanasinitt and R. Traiphol, *Journal of colloid and interface science*, 2011, **360**, 565-573.
113. G. De Las Cuevas, J. Faraudo and J. Camacho, *Journal of Physical Chemistry C*, 2008, **112**, 945-950.
114. M. Benelmekki, C. Caparros, A. Montras, R. Goncalves, S. Lanceros-Mendez and L. M. Martinez, *Journal of Nanoparticle Research*, 2011, **13**, 3199-3206.